Migration of Potassium in an Iron-based Fischer Tropsch / Zeolite composite catalyst

BY

Xoliswa Yolanda Gwagwa

Submitted to the University of Cape Town in fulfillment for the requirements for the degree

MASTERS OF SCIENCE IN ENGINEERING

December 2008

Centre for Catalysis Research

Department of Chemical Engineering

University of Cape Town

Private Bag

Rondebosch, 7701

South Africa

Declaration

I hereby:

a) grant the University free licence to reproduce the above thesis in whole or in part for the purpose of research;

b) declare that:

i) The above thesis is my own work, both in conception and execution and that apart from the normal guidance from my supervisor, I have received no part assistance apart from stated below;

ii) To my knowledge, except as stated below, neither the substance or any part of the thesis has been submitted in the past, or is being, or is submitted for the degree in the University or any other University

ACKNOWLEDGEMENTS

It is indeed a great pleasure to thank the many people who made this thesis a resounding success.

The main credit for such support, of course, should undoubtedly go to my supervisor, Eric van Steen for his inspiration, support, advice and encouragement throughout this work, mostly for his great efforts to explain things clearly and simply, and most of all for all, his good ideas I would have been lost without him. Thank you Eric for believing and for having faith in me and mostly importantly for always being there for me. It was not easy, but your support helped me through it all. This would not have been possible without you. Thank you.

Thank you to the University of Cape Town, Sasol, NRF for financial support and continued interest in the project.

To my mentor Dr Frans Prinsloo (Sasol Technology), thank you for all your help and support when I needed it the most, I am most grateful.

Thank you to the iThemba labs for making the XRD facilities available to me.

Miranda Waldron of the Electron Microscope Unit, University of Cape Town, for SEM/EDS, your patience was much appreciated

The entire Catalysis Research group, (students and staff) for providing a stimulating and fun environment for learning and growing.

Mr Kudzai Changunda for his never ending encouragement and support and for his willingness to teach and for giving me a shoulder to laugh and cry on during the difficult and happy times of my study period

Mr Nzuzo Mbuthuma for his endless encouragement and support despite the shortage of time together, nonetheless, our love and friendship have still deepened

I thank my family and loved ones for their variable support throughout the entire period but most importantly, my mother Zilungile Gwagwa for always been my pillar, my joy and my guiding light, and above all, a great source of strength throughout my studies. You turned any fears of failure into desires to succeed.

Finally I thank the almighty GOD for his guidance, wisdom, protection and his blessings.

DEDICATION

This work is dedicated to the loving memory of my Grandmother, Mrs Penelope Gwagwa.

SYNOPSIS

The product of the Fischer-Tropsch synthesis is low in aromatics and as a result has relatively poor gasoline quality (with respect to the octane number). Due to the low octane value of gasoline, extensive work-up to improve the octane number is required. Thus the cracking of longer chain hydrocarbons and the oligomerisation of light olefins may increase the yield of gasoline products. The branched and aromatic products formed from skeleton isomerisation and aromatisation reaction over acid zeolites have a high octane number.

Thus an alternative process proposed for the production of high quality gasoline from synthesis gas utilises a composite catalyst comprising of an alkali promoted iron based Fischer Tropsch (FT) catalyst and an acidic co-catalyst (ZSM-5) [Udaya et al, 1990; Schulz et al, 1991]. Therefore by using a zeolite combined with a Fischer Tropsch catalyst will result in an increase in the selectivity and quality of the gasoline range products [Botes and Böhringer, 2004, Schulz et al, 1991].

A close contact between K-promoted Fe-based catalysts with H-ZSM-5 resulted in a decrease in catalytic activity and gasoline selectivity (as defined by products in the range C_5-C_{11}) and an increase in CH_4 and light paraffin selectivity with time on stream [Botes and Böhringer, 2004]. This was ascribed to the mobility of potassium away from iron, resulting in a decrease in olefin content [Botes and Böhringer, 2004; Schulz et.al, 1991].

Thus the experimental investigation was performed using Scanning Electron Microscope (SEM) and Energy Dispersion X-ray Spectrometer (EDX), Atomic Adsorption spectroscopy (AAS) to monitor the concentration profile of iron, potassium, silicon and aluminium as a function of position in the pellet and time after heating at 350^{o}C. The pellet containing an ion exchanged H-ZSM-5

(Si/Al 40) with unpromoted iron oxide (Fe_2O_3) was pressed into a single pellet and later exposed to a temperature of 350^oC for different number of days. This was done to investigate whether iron, silicon or alumina was diffusing. But the results obtained showed that neither of these elements were mobile.

The next investigation was perfomed by pressing unpromoted iron oxide (Fe_2O_3) with potassium promoted iron oxide (6.7g K_2O/100g Fe) into a single pellet and later exposed to a temperature of 350^oC for different number of days. This was done to investigate potassium profile between two catalysts of the same crystalline structure and morphology and to see whether this can have an influence on how potassium diffuses. The conclusion that was drawn was that potassium diffuses faster between two iron oxides catalysts and after 6 days saturation was reached between the two catalysts.

This was not the case when an ion exchanged H-ZSM-5 (Si/Al 40) and potassium promoted iron oxide (6.7g K_2O/100g Fe) were pressed into a single pellet and later exposed to a temperature of 350^oC for different number of days. The most important conclusion that was drawn from this investigation was that potassium migration is governed by transport through the boundry layer of the two combined pellets. The diffusion of potassium is influenced by temperature and time of exposure in heat. After 6 days of these pellets being heated, it was observed that potassium diffusion remained constant, but no saturation was reached.

The combined pellet containing H-ZSM-5 and K/Fe_2O_3 was separated into 2 single pellets after being heated for a number of days. The HZSM-5 pellet was crushed into powder and characterised by NH_3-Temperature Programmed Desorption. NH_3-TPD was used to characterise the acidity of H-ZSM-5 which was influenced by potassium migration. The conclusion that was drawn from this investigation was that potassium migration from the promoted iron based

catalyst affected the acidity of H-ZSM-5, such that, the desorption of NH_3 adsorbed onto H-ZSM-5 changed with increasing heating time of the pellets. Thus resulting in a decrease in the acid content of the H-ZSM-5. This was due to potassium diffusing into H-ZSM-5 but after 6 days the acid content remained constant. The decrease in acid content resulted in a shift in desorption peak to lower desorption temperatures, but after 6 days stabilization in desorption temperatures was observed

TABLE OF CONTENTS

TABLE OF FIGURES

LIST OF TABLES

NOMENCLATURE

AAS	Atomic Absorption Spectroscopy
H-ZSM-5	Zeolite Socony Mobil
SEM	Scanning Electron Microscopy
NH_3-TPD	Temperature Programmed Desorption of ammonia
XRD	X-ray diffraction
EDS	Energy Dispersion X-ray Spectroscopy

1.1 INTRODUCTION

The production of synthetic liquid fuels from coal can be achieved by means of a Fischer Tropsch process. The process involves the conversion of low value coal into high value products. However there are limitations with this synfuel production route with respect to gasoline selectivity and quality. The Fischer Tropsch product spectrum consist of linear hydrocarbons [Dry, 1981]. This is a disadvantage to the gasoline quality, due to linear molecules which have a low octane number.

These limitations can be addressed by the addition of an acid catalyst (e.g. zeolite) to the process. The production of high quality gasoline from syngas can be achieved by using a bifunctional system, containing two catalytic functions. This system consists of a carbon monoxide hydrogenation function which produces hydrocarbons, most preferably highly olefinic or oxygenated compound from syngas. The Fischer Tropsch / zeolite combination process directly produces high quality gasoline, that does not require any further upgrading [Schulz, 1999].

The iron based Fischer Tropsch catalysts need alkali promotion, in which case potassium is usually imployed. A promoter is used to attain the desired activity and selectivity [Schulz,1999]. Potassium is mobile and migrates to the zeolites under normal Fischer Tropsch synthesis condition, this leads to the poisoning of the acids sites [Butter et al. 1981]. The acid sites can be prevented from poisoning by the addition of alumina which will act as a binder to trap potassium. This will results in the lowering of the potassium content of the iron catalyst, thus affecting the perfomance of the Fischer Tropsch function of the bifunctional process [Niederberger, 1988; Schulz et al. 1991].

An alkali promoted iron catalyst in combination with zeolites is the prefered choice. The iron based Fischer Tropsch catalyst can be operated at high temperatures, that are required for sufficient zeolite perfomance without producing excessive amount of methane and have product slate rich in olefins and oxygenates. The alkali promoted iron catalyst produces heavy molecules that can be cracked down to lower olefines by zeolites, undergoing aromatisation reaction. The migration of alkali from the iron catalyst is a serious concern. The problem of alkali migration from an iron Fischer Tropsch catalyst to an acid co-catalyst is discussed in literature. Its discussed in a sense that the alkali will poison the acid sites, while small amount of literature mentions the possible influence of alkali depletion on the behaviour of the iron catalyst.

A study by Botes and Böhringer on two catalysts which were physically mixed showed that the products became lighter with time on line, but the C_{5+} fraction was still rich in aromatics at the end of the run. The calculations performed confirmed that the total amount of alkali contained in the iron catalyst was not sufficient to affect the acidity of the zeolite. Therefore a conclusion was drawn that when a promoted iron catalyst was combined with a zeolite, alkali migration will only have a significant influence on the selectivity of the zeolite then the activity of the zeolite. Thus the useage of a binder such as alumina to trap potassium will not solve the problem of potassium migration for this catalyst system, as the iron phase will still have potassium depletion.

One of the objective of this study is to develop a methodology to accurately measure potassium migration most importantly to investigate the migration of potassium from the iron based Fischer Tropsch catalyst as a function of temperature and time. If the methodology proves to be correct, the introduction of a suitable barrier to inhibit migration can be investigated.

1.2 Fischer Tropsch Syntheses

Fischer Tropsch process is a polymerization reaction that takes place on the surface of the catalyst [Dry, 1981; Udaya et al, 1990]. The Fischer Tropsch process can be simplified as shown in reaction scheme (I) and (II) for the formation of long chain olefins and paraffins at 234^{o}C - 269 ^{o}C.

$$2n\ H_2 + n\ CO \rightarrow C_nH_{2n} + n\ H_2O \qquad \Delta H_r = -120 - -150\ kJ/mol \qquad (I)$$

$$(2n+1)\ H_2 + nCO \rightarrow C_nH_{2n+2} + n\ H_2O \quad \Delta H_r = -220 - -160\ kJ/mol \qquad (II)$$

In addition to these products, the Fischer Tropsch process also produces a wide range of side-products including CO_2 from water-gas shift reaction, aromatics / naphthenic compounds and oxygenated compounds which include alcohols, ketones, carboxylic acids and aldehydes. The spread of products can be influenced by a number of variables which include temperature, feed gas composition, pressure, catalyst type and promoters. The Fischer Tropsch process can be operated at two different regimes [Dry, 2002] i.e the high temperature (HTFT) and low temperature (LTFT) Fischer Tropsch system. The LTFT (220-250^{o}C) process with either Fe or Co catalyst is mainly used for the production of high molecular mass linear wax, while the HTFT (320-350^{o}C) process with Fe based catalyst is used for production of low molecular mass olefins and gasoline [Dry, 1996].

The Fischer Tropsch synthesis is a polymerization reaction which involves the sequential addition of C_1-units, hence the Fischer-Tropsch process is not selective for a product of a given carbon number range. The Fischer Tropsch process has two major disadvantages with regards to the production of gasoline. One of the main problems with the Fischer Tropsch synthesis is the carbon number distribution of the product spectrum which follows the Schulz-Flory statistical function characterized by the chain growth probability.

This however, means that the gasoline selectivity (C_5 – C_{11}) is limited to a maximum value of 48% by weight of total hydrocarbons formed. An additional drawback to the Fischer Tropsch process is the production of linear olefins and paraffins which have a low octane number. To address these problems, an acid co-catalyst, ZSM-5 can be added to the system [Schulz et al, 1991]. Thus the presence of this co-catalyst in the system resulted in highly branched and aromatic hydrocarbons of high octane value thus increasing the quality of gasoline and selectivity [Botes and Böhringer, 2004].

1.2.1 EFFECT OF TEMPERATURE ON FISCHER TROPSCH

Temperature is the most important operating parameter and by rising the temperature there is a shift to lower carbon number products and to more hydrogenated products. This occurs to a larger or smaller extent for all FT catalysts. The primary products in the FT synthesis are linear alpha olefins, paraffins, alcohols, aldehydes and carboxylic acids, these products are formed at low temperatures [Schulz et al, 1991]. But as the temperature is increased the degree of branching increases thus secondary products are formed including e.g. ketones, skeletal and double bond isomerisation and the formation of aromatics [Dry, 1981]. The formation of methane is favored at elevated temperatures, therefore the probability of chain growth decreases with increases temperature. This is due to hydrogenation resulting in a decrease in alkene ratio lowering the surface concentration of CH_2 units [Steynberg and Dry, 2004].

1.2.1.1 Catalysts for Fischer Tropsch synthesis

Group VIII metal activities were tested by Vannice [1977] in carbon monoxide hydrogenation. Only the four metals, iron, cobalt, ruthenium and nickel were found to have sufficiently high activity for the hydrogenation of carbon monoxide for Fischer Tropsch synthesis [Dry, 2002; 2004].

1.2.1.1.1 Nickel

When nickel was used as a Fischer Tropsch catalyst it was found to produce relatively high methane selectivity because it is a stronger hydrogenating catalyst when compared to e.g. iron and cobalt. Thus nickel was abandoned as a FT catalyst [Dry, 2004].

1.2.1.1.2 Ruthenium

With ruthenium as a catalyst very high molecular mass waxes are produced at low temperatures and high pressures (170^{o}C) whereas at high temperatures (400^{o}C) only methane was produced. The price of ruthenium is very high therefore because of this limitation ruthenium was abandoned as a FT catalyst leaving only cobalt and iron as practical catalysts [Dry, 1996].

1.2.1.1.3 Iron and Cobalt based Fischer Tropsch catalyst

From the above statements it is clear that only cobalt and iron based catalysts can be considered as practical Fischer Tropsch catalysts for commercial application [Dry, 1996]. Cobalt operates at low temperatures (220 – 250^{o}C) producing water as a co-product in hydrocarbon synthesis. Iron is usually operated in two ranges of temperatures, at low temperatures of (220 – 250^{o}C) and high temperatures of (320 – 350^{o}C,) [Dry, 1981]. Cobalt is a more active hydrogenating catalyst then iron therefore methane selectivity increases strongly with temperature for cobalt based catalyst than it with iron based catalyst. Fischer-Tropsch synthesis over cobalt-based catalysts results in a product distribution with more paraffins than that of an iron-based catalysts, [Dry, 2002].

Olefin readsorption on the FT site does take place over cobalt based catalyst, resulting in the significant contribution of the high wax selectivity which is hydro-cracked to obtain diesel fraction, [Schulz and Claeys, 1999]. Since cobalt and ruthenium as Fischer Tropsch catalysts have very high methane selectivity at high temperatures, they are not expected to be effective in the bifunctional process [Schulz et al, 1991]. An increase in methane formation with an increase in temperature is less excessive for an iron based catalyst, then when compared to cobalt and ruthenium based catalyst [Schulz, 1999]. Highly olefinic product spectrum can be achieved with an iron based catalyst, thus an iron based catalyst is the catalyst of choice. However an iron catalyst needs to be promoted by an alkali promoter to attain the desired activity and selectivity [Botes and Böhringer, 2004].

1.3 Alkali Promoters

Promotion with alkali metals in industrial practice is one of the important ways of influencing the properties of catalysts either their activity or selectivity. The addition of a small amount of promoter has a great effect on selectivity and activity [Narkiewicz et al, 2005]. For iron based FT catalyst, the addition of strong alkali chemical promoters is important for achieving satisfactory activity most importantly achieving the desired product spectrum [Dry, 1991]. Iron is more responsive to promoters such as potassium (K_2O) than cobalt or nickel. The promotion of all Fe catalysts with an alkali, such as the potassium salt is important for the Fischer Tropsch selectivity and activity [Dry, 2002].

Potassium on the catalyst surface increases electron density, resulting in the formation of unsaturated products which include olefins and oxygenates. The basicity of the promoted catalyst does not only depend on the amount of the alkali added but it also depends on the interaction with other components that might be added or present in the system (SiO_2, Al_2O_3). The alkali will interact with these components forming less acidic compounds.

Potassium has been used as a promoter for an iron catalyst to increase the alkene yield and to decrease the amount of methane in the product. A study done by Luo and Davis, (2003), indicated that an iron based catalyst operating at temperatures of 330^0C will yield approximately ca. 40% methane, but when promoted with a small amount of potassium the methane selectivity was observed to drop to ca.10%.

The presence of other compounds regardless of whether they were added or present as impurities can have a strong influence on the effectiveness of the alkali promoter. For example if silica is present in the system, the alkali will react with Si to form alkali-silicate which will be less basic than the free alkali and thus the basicity of the iron surface will be lowered. A similar reaction will occur in the presence of alumina to form less basic aluminates. If there is no chemical interaction between the promoter and the support material, alkali will be diluted in such a way that it will not only be distributed on the iron surface but also on the surface of the other component. This means that the amount of alkali to be added must be adjusted taking to account the chemical nature and the surface area of components that are present [Steynberg and Dry, 2004].

With increasing alkali the high chain growth probability and activity passes a maximum as a function of alkali content [Steynberg and Dry, 2004]. The higher the carbon concentration on the surface the high the coverage by CH_2 building blocks and thus the higher the probability of chain growth. Potassium can increase both FTS and water gas shift catalytic activity and attain the desired selectivity [Eliason and Bartholomew, 1999]. A study by Luo and Davis (2003) on the effect of a potassium promoter on the product selectivity and CO conversion over an iron-based Fischer-Tropsch catalyst comparing it to the unpromoted catalyst showed that the olefin content in the C_2-C_4 fraction increased significantly by the addition of potassium, especially in C_2. The chain growth probability of the promoted catalyst was also found to be higher.

Potassium can increase both Fischer Tropsch synthesis and water gas shift catalytic activity and attain the desired selectivity [Eliason and Bartholomew, 1999].

1.4 ZEOLITES

Zeolite is an important class of material that have found extensive use as catalysts, catalyst support and ion exchangers. These are characterized by framework structures which consist of uniform pore and channel systems [Breck, 1974]. They are characterized as small, medium or large pore zeolites and the performance of acid zeolite can be influence by silica to alumina ratio.

Zeolites posses unique properties based on their crystalline aluminosilicate material. These properties include: [Maxwell and Stork, 2001; Haag et al, 1987]

- ion-exchange properties
- microporous character, allowing certain hydrocarbons to enter the zeolite core system and reject other molecules based on molecular size
- high thermal stability
- high hydrothermal stability
- acidity

1.4.1 Zeolite structures

In zeolite's framework, the silicon and aluminium atoms are referred to as T atoms, thus the framework density of zeolite is normally expressed as T atoms per 1000Å^3 which in turn is the measure for the void volume. Zeolites are classified according to the number of T atoms in the rings that form the structure of the channels. Structural channels of zeolites range from very small (8T atoms) to very large pore zeolites up to 20 T atoms.

These channel system may be one-dimensional (e.g.ZSM-12), two-dimensional (e.g. MCM-22) or three-dimensional (e.g. Beta), these can interconnect or be independent on each other. ZSM-5 contains one-dimensional channel systems which contain different orientations. These interconnect such that the total channel system is three-dimensional [Baerlocher, et al, 2007].

Most number of zeolites may undergo dehydration to a certain degree without major alteration of their crystal structure. Upon complete dehydration, many zeolites undergo irreversible structural changes and complete structural collapse. For some zeolites a complete dehydration results in irreversible changes in framework topology because of the framework having weaker linkages in certain direction. Thus the exchangeable cations that are initially located in the channels may be trapped [Breck, 1974].

1.4.2 STABILITY AND ACIDITY OF ZEOLITES

There are several factors which are known to affect the thermal behavior and stability of zeolites material. The ratio of Si/Al is amongst the most important factors. An increase in Si/Al ratio results in an increase in thermal stability, because more energy is required to break the Si-O bond when compared to Al-O bond. The same reasoning applies for the increase in acid resistance with increasing Si/Al ratio. The high stability of zeolites is generally attributed to their high silica content [Cruciani, 2006].

Zeolites are tetrahedrally bound silicon and aluminium ions which are joined by bridging oxygen ions. A negative framework charge that is induced by the tetrahedral coordination of aluminium is neutralized by the presence of exchangeable cations. This charge compensation effect is responsible for the acidity and activity of zeolites.

The synthesis of zeolites results hypothetically in a sodium form, which is later replaced by ammonium cations. Upon heating, ammonia is released from an ammonium-exchanged zeolite, resulting in an active proton being formed. The number of acid sites in zeolites is proportional to the number of aluminium in the framework.

1.4.3 Zeolite ZSM-5

The pore channels and dimensions are in an order of nanometer (1nm = 10Å) and the diameter of the cylindrical pore and channel of a zeolite ZSM-5 is about 5.5Å [Raksakoon and Limtrakul, 2003]. ZSM-5 zeolite is one of the important nanostructured catalysts for petrochemical and hydrocarbon processing because of its unique characteristics involving shape and size selectivity, thermal stability and acidic nature [Raksakoon and Limtrakul, 2003].

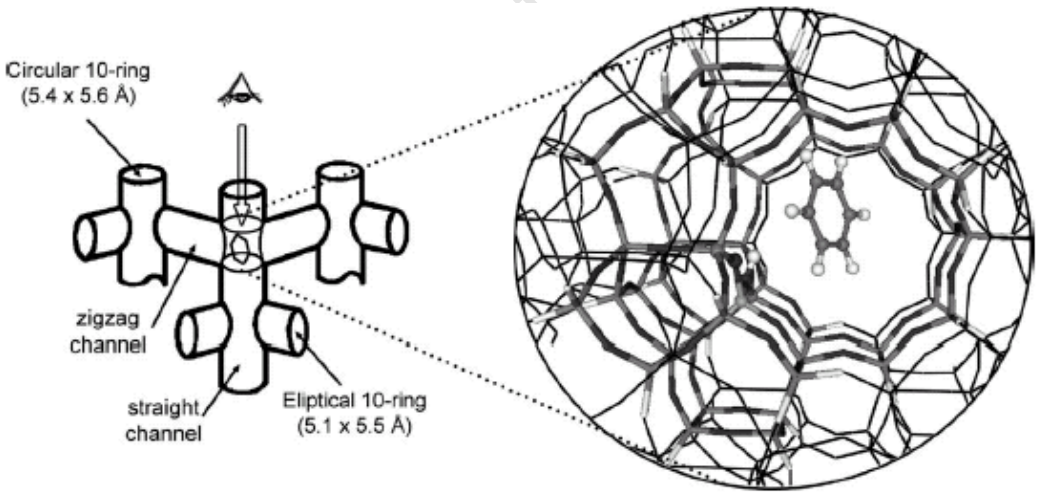

Figure 1.1: The Structure of H-ZSM-5 showing three different channel structures [Raksakoon and Limtrakul, 2003]

Fig.1.1 shows the structure of ZSM-5 which is viewed from the top view of the straight channel intersection; ZSM-5 has two different channel structures of H-ZSM-5, which include the channel intersection, the straight channels and the zigzag channels. The straight channels have dimensions of 5.4 x 5.6Å, the zigzag channels have dimensions of 5.1 x 5.5Å. The intersection channels are modeled by the 46T cluster and have a spatial dimension of about 9Å [Raksakoon and Limtrakul, 2003].

Figure 1.2: Channel intersection cavities [Fraenkel et al, 1984]

1.4.3.1 Shape and size selectivity

The internal surface of ZSM-5 plays a major role in shape selective catalysis. ZSM-5 is a medium size pore zeolite. The main factor that allows molecular sieving is the shape selectivity which is considered as a sterical effect therefore only molecules with a certain diameter are allowed to enter the pores and react on the active site or exit thereby recovered as products. Larger molecules in the reaction or product mixture will have greater diffusional resistances inside the channels then smaller molecules.

The formation of aromatic with a carbon number above C_{10} is avoided in the production of high octane gasoline [Armaroli; et.al, 2006]. The shape selective properties of ZSM-5 limit the formation of polycyclic aromatics inside the pores and cavities of the crystals [Botes, 2005]. Lastly the medium pore size of the zeolite makes it resistant to coking because of its three dimensional structure. [Armaroli et al, 2006].

1.4.3.1.1 Experimental observations of shape selectivity

A study by Haag et al (1987) involved a number of catalytic cracking reactions over ZSM-5. The cracking of various hydrocarbons compounds was compared over small crystal and large crystal ZSM-5. This was achieved by calculating the rate constant and the effective factor in each case. The following conclusions were made:

- There is no mass transport of diffusional effect at cracking temperatures of 323-523^{o}C, since the cracking rate of paraffins (alkanes) and monomethyl paraffins are independent of crystal size
- There is a rise in mass transport effect in large crystals because of diffusional resistance.
- Diffusivity and reaction rate is slightly affected by the total length of the molecular chain
- Bulkier molecules have difficulty diffusing into the channels of the catalysts, because the reaction rate drops significantly in larger crystals.

The medium size channel of ZSM-5 allows for the diffusion of small aromatic molecules and linear hydrocarbons, but the motion of larger molecules is restricted. Fraenkel (1984) proposed that the ZSM-5 has two types of catalytic sites. The first type is located inside the crystal and the second one resides on the external surface of the zeolite and is not shape selective.

Thus a conclusion can be drawn that the internal surface of ZSM-5 plays a role in shape selective catalyst and the effect of the external surface is less certain. Larger molecules in the reaction or product mixture will have great diffusional resistances inside the channel then when compared to smaller molecules [R. Weber, 1993].

1.5 Catalytic Function of Fischer Tropsch catalyst

The two most important disadvantages of the Fischer Tropsch process with regards to the production of gasoline are:

1. The carbon number distribution of the product spectrum, which results in the selectivity of gasoline (C_5-C_{11}) to be limited to a theoretical maximum value of about 48%
2. Fischer Tropsch process produces mainly linear olefins and paraffin. These compounds have a low octane value, resulting in an extensive gasoline work up, to improve the octane number [Dry, 1981].

These two disadvantages can be addressed by the addition of an acid co-catalyst to the system [Schulz and Niederberger, 1991]. To increase the gasoline yield, the long chain hydrocarbons must undergo cracking and there must be oligomerisation of light olefins. Branched and aromatic hydrocarbons are formed from skeletal isomerisation and aromatisation reactions over acidic zeolites. Therefore products formed have high octane values. The use of a zeolite in combination with a Fischer Tropsch catalyst can result in an increase in both the selectivity and quality of gasoline [Botes and Böhringer, 2004].

1.5.1 Bifunctional catalyst for syngas conversion

The production of high quality gasoline directly from a bifunctional system contains two catalytic functions. Firstly there is hydrogenation of carbon monoxide producing hydrocarbons i.e highly olefinic and oxygenated compounds from syngas. Secondly an acid catalysed function such as a shape selective zeolite which converts the olefinic or oxygenate hydrocarbons to gasoline fraction which is rich in aromatics, naphthenes and branch aliphatics [Botes, 2004]

1.5.1.1 Consideration of Fischer Tropsch function

The following Fischer Tropsch characteristics are vital for a bifunctional process:

- The formation of light paraffin should be avoided; this can be achieved by reducing the selectivity of methane. Light paraffins have low fuel value and cannot be easily converted to gasoline range components or other useful products.
- There must be a high selectivity for olefins and oxygenates, because these compounds have low hydrogen to carbon ratio then paraffins and they are very reactive over zeolites.

For a desired hydrocarbon reaction to be achieved over zeolite catalysts, the reaction temperature has to be above 300^{o}C [Muller et al, 1982].

1.5.2 Zeolite Function

The most important aim for bifunctional process is to produce high octane gasoline selectivity [Udaya et al, 1990].

- ZSM-5 has medium size pores, thus formation of aromatic compounds above C_{10} is avoided.
- H-ZSM-5 is highly acidic therefore the oligomerisation, isomerisation, cracking and aromatisation reactions can be catalysed effectively.
- The medium size pore prevents the formation of larger molecules that can act as coke precursors. Thus ZSM-5 has a high resistance to coke formation.
- ZSM-5 is stable under hydrothermal conditions. Under Fischer Tropsch conditions it's resistant to dealumination.

The acidity of H-ZSM-5 is dependent on silica/alumina ratio, this influences the performance of the zeolite. The silica/alumina ratio of the zeolite can be varied and has a significant influence on the performance of catalyst [Horsley et al, 1993]. The number of acid sites increases with increasing aluminium content of the zeolite therefore resulting in an increase in octane value of the product. The silica/alumina ration has a major influence on the selectivity and activity of the bifunctional process. It also has an influence on the coking of zeolite. Thus there should be optimum aluminium content of the H-ZSM-5 for application in the bifunctional process. This optimum depends on the product spectrum produced by the Fischer Tropsch function together with the process conditions [Botes, 2004].

1.5.2.1 Coke formation and deactivation of zeolite

The small aromatics formed in the channels of H-ZSM-5 can diffuse with ease out of the zeolite channels due to the intersecting channel systems of the zeolite. ZSM-5 does not deactivate extensively due to coke formation in the channels. However when the coke formation on the external surface becomes dominant, the poly-aromatic molecule on the external surface will block the access to the channels. Thus the deactivation of ZSM-5 is caused by the coverage of the external surface.

The loss in activity of zeolite may be caused by the formation of coke, which is expected for an acid zeolite in HTFT environment resulting in deactivation of the zeolite due to coke formation. The formation of coke is a shape selective reaction thus the zeolite structure has a great influence on the formation of coke. Schulz et al (1987) reported that the coke found in the channels of H-ZSM-5 consisted of alkylated 2-ring aromatics, although the nature of the coke may depend on the feed. The coking rate is greater when the cavities or channel intersections are great.

The higher synthesis temperature has a direct influence on the product spectrum resulting in a shift towards light hydrocarbons and lower olefins. But there is an indirect influence on the product spectrum as it directly enhances the rate of carbon formation by the iron FT catalyst. Coke formation on the H-ZSM-5 can be influenced by a number of factors. Operation temperature has a very strong influence on the type and location of coke formed and the coking rate. The ratio of external to internal coke deposition increases and the aromaticity of the carbonaceous deposits increase with the enhancement of polycyclic aromatic compounds by increasing the synthesis temperature. This can be explained by the shape selectivity properties of H-ZSM-5, which limits the formation of polycyclic aromatics inside the pore and the cavities of the crystals.

Thus the coke inside the crystal consists of large aliphatic compounds and monocyclic aromatics with bulky alkyl side chains. These molecules cannot diffuse out of the zeolite pores thus they become trapped inside the crystals and restrict access to the pores and cavities. Higher temperature promotes the formation of polycyclic aromatics on the external surface of the zeolite. Therefore an increase in temperature decreases the rate of coke formation inside the crystal, but increases coke formation on the outer surface [Botes, 2005].

According to literature, there is an optimum operating temperature where the overall rate of coke formation is low. It's been reported that the lowest rate of coke formation during hydrocarbon formation over H-ZSM-5 occurs at temperatures of 350-370^{o}C. The rise in the operational temperature of the bifunctional process from 330 to 350^{o}C is expected to result in a lower rate of deactivation of the H-ZSM-5 co-catalyst [Botes, 2005].

1.6 Influence of Two Catalytic Functions on each other in a Bifunctional Process

A study by Botes and Böhringer (2004) aimed at investigating the viability of a single step bifunctional process whereby the two catalytic functions would be in the same reactor. This was done to achieve the desired hydrocarbon reactions over zeolite catalysts at temperature above 300^{o}C in a Berty microreactor. A combination of an alkali promoted iron catalyst and an acidic co-catalyst was used for this study. Intimate contact between the two catalysts of the bifunctional process had an effect on the performance and selectivity of the iron catalyst.

A close contact between K-promoted Fe-based catalysts with H-ZSM-5 resulted in a decrease in catalytic activity and gasoline selectivity (as defined by products in the range C_5-C_{11}) and an increase in CH_4 and light paraffin selectivity with time on stream [Botes and Böhringer, 2004]. This was ascribed to the mobility of potassium away from iron, resulting in a decrease in olefin content thus forming light paraffins that cannot be converted to higher value products by employing a zeolite, therefore resulting in an increase in methane selectivity [Botes and Böhringer, 2004; Schulz et.al, 1991].

1.6.1 Effect of Higher operation Temperature on Two Catalytic Function on a Bifunctional Process

Botes (2004) investigated the influence of higher temperature (350^{o}C opposed to 330^{o}C) on the product distribution of the bifunctional process. The lifetime of the zeolite co-catalyst has shown that there is no optimization of the performance of an iron catalyst at higher temperatures. Temperature can have an indirect influence on the product distribution since there is an enhancement in the rate of carbon formation by the iron FT catalyst.

Alkali which is a promoter undergoes migration under synthesis conditions to the carbon deposited on the catalyst. This results in the alkali level of the active iron phase to decrease resulting in a shift on the product spectrum towards lighter and more paraffinic products and thus an increase in methane selectivity. This results in the selectivity of the desired product being gasoline to decrease at higher synthesis temperatures.

1.6.2 Diffusion of Potassium

For an iron based Fischer Tropsch catalyst to achieve a desired activity and selectivity it requires an alkali promoter, usually potassium is used [Schulz, 1999]. Under normal Fischer Tropsch synthesis conditions, potassium is mobile and migrates to the zeolites, thereby lowering the content of potassium in the iron catalyst. This inturn affects the perfomance of the Fischer Tropsch function of the bifunctional process [Niederberger, 1988, Schulz et al, 1991]. The physical mixture of H-ZSM-5 with FT catalyst resulted in an increase in methane selectivity, therefore the bifunctional process seems to be an unfeasible option due to low selectivity of desired gasoline range product.

Alkali migration from the FT catalyst to an acidic catalyst is discussed in literature from the perspective that the alkali will poison the acid site, resulting in the loss of acid catalyst activity. Little is mentioned on the possible influence of alkali depletion on the behaviour of the iron catalyst. Based on the experiment that was performed on two catalysts in physical admixture, it was concluded that alkali migration would have more infleunce on the selectivity of the iron catalyst, then on the activity of the zeolite [Butler et al, 1981].

The surface diffusion of alkali metals is affected dramatically by surface cleanliness and surface anisotropy. A study by W. Zhao, et al. (2000) address the effect of an ionic oxide substrate [Cr_2O_3(0001)/Cr(110)] on the interaction and surface diffusion of potassium. They reported the diffusion of alkali-metal atoms on oxide surfaces over distances of several micrometers. Whereby the activation energy of surface diffusion of potassium on Cr_2O_3(0001)/Cr(110) was determined to be 11 $\pm$ 0.5 kcal/mol with a pre-exponential factor $D_o = 10^5$ cm^2/sec in the coverage range of 1.5-2.5 ML. There was a drop in activation energy to 9 kcal and $D_o = 3 \times 10^3$ cm^2/sec at a coverage range of 3.0 ML[Zhao, et al, 2000].

A study by Danzinger et al (2004) focused on the effect of coadsorbed CO on the diffusion of potassium. They reported that the amount of CO coadsorbed on K/Ru(001) controled the surface diffusivity of potassium by forming more then one type of K_y - CO_x surface complex. CO and potassium attraction resulted in an increase in the activation energy from 2.7 kcal/mol on a clean metal, to 17.0 kcal/mol and an increase in pre-exponential factor from 8.3 x 10^{-8} to 3.1 x 10^{-1} cm^2/s for the surface diffusion of potassium on Ru(001).

Diffusion coefficient is expressed in an Arrhenius form [Danzinger et al, 2004]:

$D = D_0 \exp(-E_{diff} / RT)$ cm^2/s

Where:

E_{diff} activation energy for diffusion

D_0 pre-exponential factor

There is a stabilization effect between coadsorbed CO and potassium through the formation of K_y - CO_x surface complexes. The composition of these complexes changes with changes in the conditions in CO coverage [Danziger et al, 2004]. Westre et al concluded that the interaction between potassium and CO forming complexes that have a 1:1 ratio is the one formed on the surface because of it being the most stable. The formation of a complex which acts as site blockers for potassium atoms, results in the thermal diffusion of potassium on the surface to be slowed down. The diffusion coefficient increased by 12 orders of magnitude for maximum CO to K ratio, whereas for clean potassium there was an increase of only 2 orders of magnitude for the same temperature range [Danziger et al, 2004].

A study by Narkiewicz, et al, (2005) on surface diffusion of potassium on iron surface which was modified by oxygen and or nitrogen, showed that the diffusion coefficient for surface covered in nitrogen (22 x 10^{-8} cm^2/s) was

smaller then that of surface covered with oxygen (25 x 10^{-8} cm^2/s). Narkiewicz; et al, (2005) concluded that potassium is stable at higher temperatures in the presence of oxygen atoms, but it was also demonstrated that nitrogen atoms on the surface of the iron oxide can stabilize potassium atoms. A conclusion that can be drawn from these studies is that the diffusion of potassium on metals is difficult, the diffusion on CO is easy and diffusion on oxide is facile.

1.7 RESEARCH OBJECTIVES AND HYPOTHESIS

Based on the study by Schulz et al (1991) and Botes et al (2004) that a close contact between a K-promoted Fe-based catalyst and H-ZSM-5 leads to:

- decrease in catalytic activity
- decrease in gasoline selectivity
- increase in methane selectivity
- increase in light paraffin selectivity

Dry (2004) in agreement with Schulz et al (1991) and Botes et al (2004) found that the migration of potassium away from iron leads to:

- decrease in FT-activity
- increase in methane selectivity
- decrease in olefin content

For these reasons it has been hypothesized that:

- the mobility of potassium is phase boundary dependent, i.e. mass transfer across the boundary layer can affect the mobility of potassium
- the mobility of potassium is reaction condition dependent, since it may affect the mobility of potassium across the boundary phase.
- the mobility of potassium is affected by both the surface migration and the interparticle migration

The objective of this study is to develop a simple methodology to investigate the mobility of potassium in K-Fe/H-ZSM-5 system.

The study will be divided into stages:

- development of methodology for measurement of potassium migration under reaction conditions using pellets

- EDX-profiling of K at a given time in a pellet initially containing an iron phase promoted with potassium and the same iron phase without potassium (Fe_2O_3) heated at 350^{o}C for a number of days
- EDX profiling at a given time in a pellet containing an iron phase promoted with potassium and a H-ZSM-5 heated at 350^{o}C for a number of days
- Profiling using NH_3-TPD at various heating times

2. Experimental procedures

2.1 Preparation of Iron Oxide

Iron oxide Fe_2O_3 was prepared by precipitation from an iron nitrate solution. For this purpose, 126.4 g of iron (III) nitrate [$Fe(NO_3)_3.9H_2O$;99%; Aldrich] was dissolved in 126 ml distilled water and heated to 90°C. In a separate beaker 295g ammonium carbonate [$(NH_4)_2CO_3$, Saarchem] was dissolved in distilled water (900ml) and was heated to 60°C. The warm ammonium carbonate solution was poured into 60^oC iron nitrate solution with continuous stirring at 60rpm using IKA 25 Basil Altra Turrax disperser with S25N-25G dispersion element for 15 minutes on a 60^oC hotplate.

The precipitate was filtered and washed with 4litres of boiling distilled water until the aqueous extract contained no nitrates. The test for the presence of nitrate involved the addition of 1ml concentrated $FeSO_4$ solution into 10ml aqueous filtrate of the original mixture in a 50ml beaker, concentrated H_2SO_4 (1ml) was poured carefully drop wise on the side of the beaker. A brown ring which is an indication of nitrate ions being present was not observed. Therefore the resulting precipitate contained no nitrates.

The precipitate was placed into a porcelain dish and dried in an oven for 16 hours at 120^oC. The dried product was crushed to 40-125μm using a mortar and pestle and calcined in air at 350^oC (flow rate 270ml (STP)/min/g; heating rate 10^oC/min) for 8 hours, in a fluidised bed reactor. The final product was stored in a desiccator.

2.1.1 Impregnation of potassium on iron oxide.

Iron oxide was subsequently impregnated by incipient wetness technique with an aqueous solution of KNO_3 (Sigma) to achieve 6.7g K_2O/100g Fe. The amount of water used for incipient wetness impregnation equalled the pore volume of iron oxide. The pore volume was estimated by drop-wise addition of water using a burette on 1g of calcined precipitate, until the level of water is just above the solid. The final volume of water added to 1g of Fe_2O_3 was estimated to be 1ml. Thus, 1ml of 1M KNO_3 solution per gram of precipitate was used for impregnation. 1M KNO_3 was dissolved in water to form a solution, which was added to Fe_2O_3 for impregnation.

The impregnated material was subsequently dried in a Rotary evaporator (Buchi Rotavapor R-205), at 80^{o}C, 250mbar and 60rpm. The rotary evaporator was kept at these conditions for 100 minutes to dry the catalyst. The dried impregnated catalyst was calcined at 350°C (flow rate 270 ml (STP)/min/g; heating rate of 10°C/ minute) for 8hours in air, in a fluidised bed reactor to remove all traces of nitrates.

2.1.2 Ion Exchange of Zeolite ZSM-5

Zeolite ZSM-5 milled powder (Süd Chemie (PTY) Ltd) was ion exchanged into H-ZSM-5 (Si/Al = 40) by performing 3 cycles of ion exchange in order to ensure removal of all Na^{+}-ions with ammonium ions. ZSM-5 (10g) powder (Süd Chemie) was ion exchanged by the addition of 100ml solution of 1M ammonium nitrate (Kimix). The mixture of ZSM-5 powder and ammonium nitrate was stirred and heated at 90^{o}C on a hot plate for 24 hours under reflux. The catalyst was then filtered and washed with 600ml of cold distilled water. The resulting product was then dried for 24 hours in an oven at 120^{o}C, and subsequently calcined at 425^{o}C in air (flow rate 270 ml (STP)/min/g; heating rate 10^{o}C/min/g) for 16 hours, in a fluidised bed reactor. The same procedure

was repeated twice for the same product using each time fresh ammonium nitrate solution. The final product was then stored in a desiccator.

2.1.3 Pellets Formation

A 1:1 ratio of potassium promoted K-Fe_2O_3 (6.7g K_2O/100g Fe) and H-ZSM-5 (Si/Al = 40) were pressed into a single pellet with a diameter of 15mm. 1g of H-ZSM-5 was pressed for 30 seconds and 1g K-Fe_2O_3 powder was pressed on top of the pressed sample of H-ZSM-5 at a pressure of 2 tons for 2 minutes, using a Specac pellet presser. Pellets containing 1g K/Fe_2O_3 and 1g H-ZSM-5 were heated in a 350^{o}C furnace for a certain number days (up to 30 days). Figure 2.1 shows the schematically the process of pellet formation.

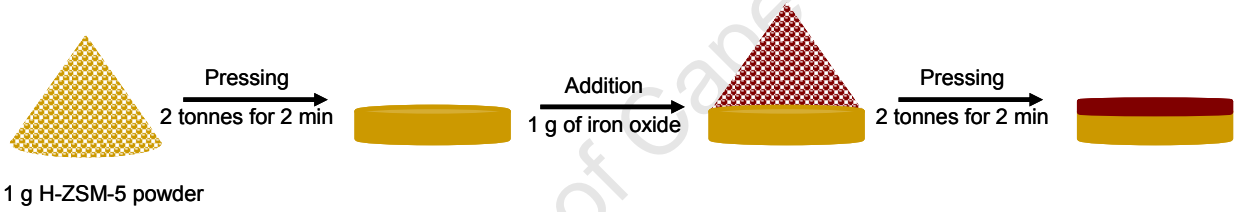

Figure 2.1: Pelletisation Methodology

2.2 Catalyst Characterisation

The materials were characterized using Atomic Absorption Spectroscopy (AAS), X-ray diffraction (XRD), Scanning Electron Microscope (SEM-EDX) and NH_3-Temperature Programmed Dessorption (NH_3-TPD).

2.2.1 Atomic Absorption Spectroscopy (AAS)

A Varian Spectra AA-30 spectrometer attached to a DS-15 station was used to determine the concentrations of iron, potassium, sodium and aluminium on the calcined potassium promoted Fe_2O_3 and H-ZSM-5 catalysts.

Determination of Fe and K content in iron based sample

10ml of a mixture containing 4 parts hydrochloric acid (40%) and 1 part hydrofluoric acid (30%) by volume was added to 0.1 g of catalyst sample in a 250 ml Erlenmeyer flask. The solution was then heated and after the solution started boiling 10 ml of 60% nitric acid was added. The resulting solution was reduced to approximately 2ml in volume by boiling off excess liquids. 5 ml of concentrated perchloric acid was added and resulting solution was reduced again to 2 ml by boiling off excess liquids. A white cloud was formed which rose once the reaction had taken place. The sample was transferred to a 100 ml volumetric flask and made up to a volume of 100 ml with distilled water. The resulting concentration of iron and potassium in this solution was determined using AAS.

Determination of Al and Na content in H-ZSM-5

0.02g of an ion exchanged sample (H-ZSM-5) and 4ml 40% hydrofluoric acid were added in a Parr bomb, and left for 2 hours at room temperature. After 2 hours the sample was quantitatively transferred to a 50 ml volumetric flask and made up to a volume of 50 ml with distilled water. The resulting aluminium and sodium concentration in the solution was measured using AAS.

2.2.1 X-Ray Diffraction (XRD)

X-ray analysis was used to analyze crystalline phases and average crystallite sizes of catalysts for prepared iron oxide product. X-ray diffraction measurements were done on a Phillips PW 3830 X-ray diffractometer with Cu-Kα radiation. All diffraction patterns were recorded in the step-scan method with the following operation settings:

- Voltage 40kV
- Current 25mA
- 2θ range 15° - 90°
- Step size 0.04 °
- Scan rate 0.7°/min

XRD patterns of powder samples are measured using stationery X-ray source usually Cu Kα and a movable detector which scans the intensity of the diffracted radiation as a function of the angle 2θ between the incoming and the diffracted beams. Powder samples give images of diffracted lines because of the small fraction of the powder particles will be oriented such that a certain crystal plane is at a correct angle θ with the incident beam for constructive interference. Rotation of the powder during measurements enhances the fraction of particles that contributes to the diffraction pattern.

Diffraction patterns from catalyst characterisation are used for crystallographic phases that are present in the catalyst. Diffraction peaks of crystalline phases were assigned by comparing to those of standard compounds reported in the Joint Committee on the Powder Diffraction Standards (JCPDS) data file. When X-rays are directed on the particle, they are diffracted by ordered planes yielding a pattern unique to a specific plane.

The Debye-Scherrer method for determining an average crystallite size $d_{c\text{-}XRD}$ involved determining the peak width at half height:

$$đ_{c\text{-}XRD} = \frac{k\lambda}{\beta.\cos\theta}$$

Where:

- $dc\text{-}_{XRD}$ Average crystallite size (nm)
- k Shape factor (constant = 0.9)
- λ X-ray wavelength (1.54 Å)
- β peak width at half maximum intensity (radians)
- θ Diffraction angle in degree

2.2.2 *Scanning Electron Microscope (SEM) and Energy Dispersion X-ray Spectrometer (EDS)*

Electron Microscopy is a straight forward technique that is used to determine the size and shape of particles. Information on the composition and the internal structure of the particles can be revealed. Depending on the thickness of the sample, a fraction of electrons passes through the sample without energy loss. The attenuation of the beam depends on the density and thickness of the sample. In SEM the electron beam is passed over the sample surface and the yield of backscattered or secondary electron is detected as a function of the position in the primary beam. The secondary electrons have a low energy (≈ 5 to 50 eV), and they carry information about the composition of the sample.

A scanning electron microscope (LEO S444 SEM, La:Ka, UK) equipped with a Four Quadrant Back Scatter Detector and an energy dispersive Fissons Kevex X-ray spectrometer (EDS) with sigma analysis software was used to monitor the concentration profile of iron, potassium, silicon, aluminium as a

function of the position in the pellet and time of heating at 350°C. The samples were prepared by mounting a combined pellet which was cut vertically in half (such that the combination of both catalysts is contained) onto stubs made of aluminium. These stubs were coated with glue containing graphite. Graphite is used to conduct electrons thereby preventing charge build up.

The penetration depth of the electrons can be estimated for energies in the range of 20keV using an equation from Kevex International Corp, Analytical Instrument Division:

$$R = \frac{4120}{p} E^{(1.265-0.0954 \ln E)}$$

Where:

R	Penetration, microns
E	Primary electron energy, MeV
ρ	Absorber density g/cm^3

2.2.3 *Temperature Programmed Desorption of Ammonia (NH_3-TPD)*

Temperature programmed desorption of ammonia was used to characterise the acidity of H-ZSM-5. It was also used to determine the number of acid sites in ZSM-5 which had been in contact with K/Fe_2O_3 at 350°C for a certain time. For this purpose the pellets were separated and H-ZSM-5 was crushed into powder and characterised using NH_3-TPD apparatus. The gasses were passed though a packed bed of catalyst in a quartz tube. The gas flows were controlled with calibrated mass flow meters. The equipment used for temperature programmed desorption studies consisted of gas lines, quartz

TPD cell, the furnace and a detector (see Figure 2.2).

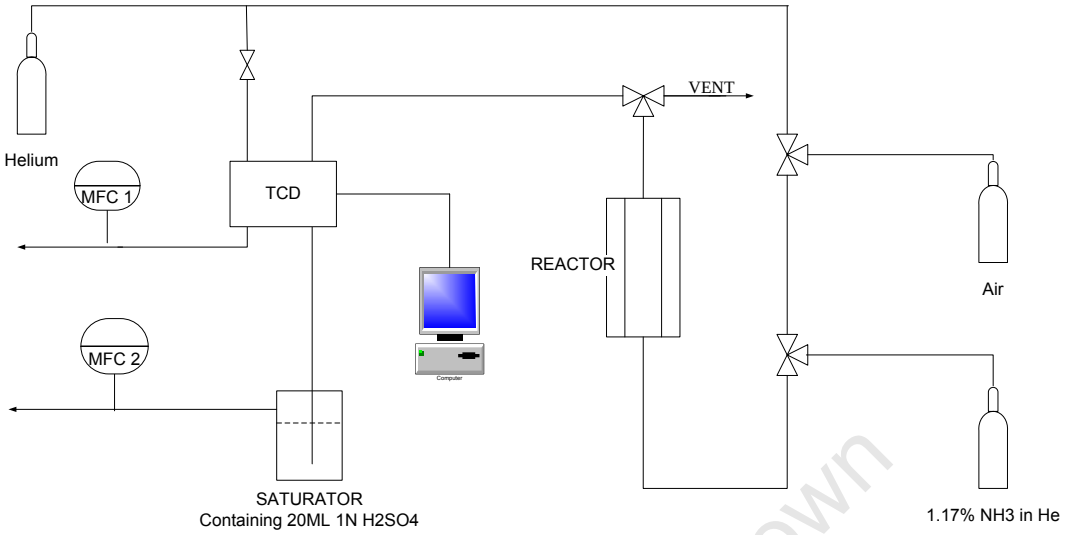

Figure 2.2: NH_3-Temperature Programmed Desorption Rig

Air, helium and a mixture of ammonia in helium were used. Air was used for calcination of the sample to ensure complete removal of all organic material, which may have been adsorbed on to the material. Helium was used during desorption stage and the NH_3/He mixture (1.17% NH_3) was used to adsorb NH_3 onto the catalyst. The gas flow was monitored and controlled using a mass flow controller which was calibrated for He, Air, the NH_3/He-mixture prior to use.

Figure 2.3 shows schematically the quartz reactor used in the NH_3-TPD experiments. The TPD cell is a 350mm long, 10mm I.D, and 12.7mm O.D quartz tube. The sample was positioned to the middle of the furnace and kept in place using quartz wool.

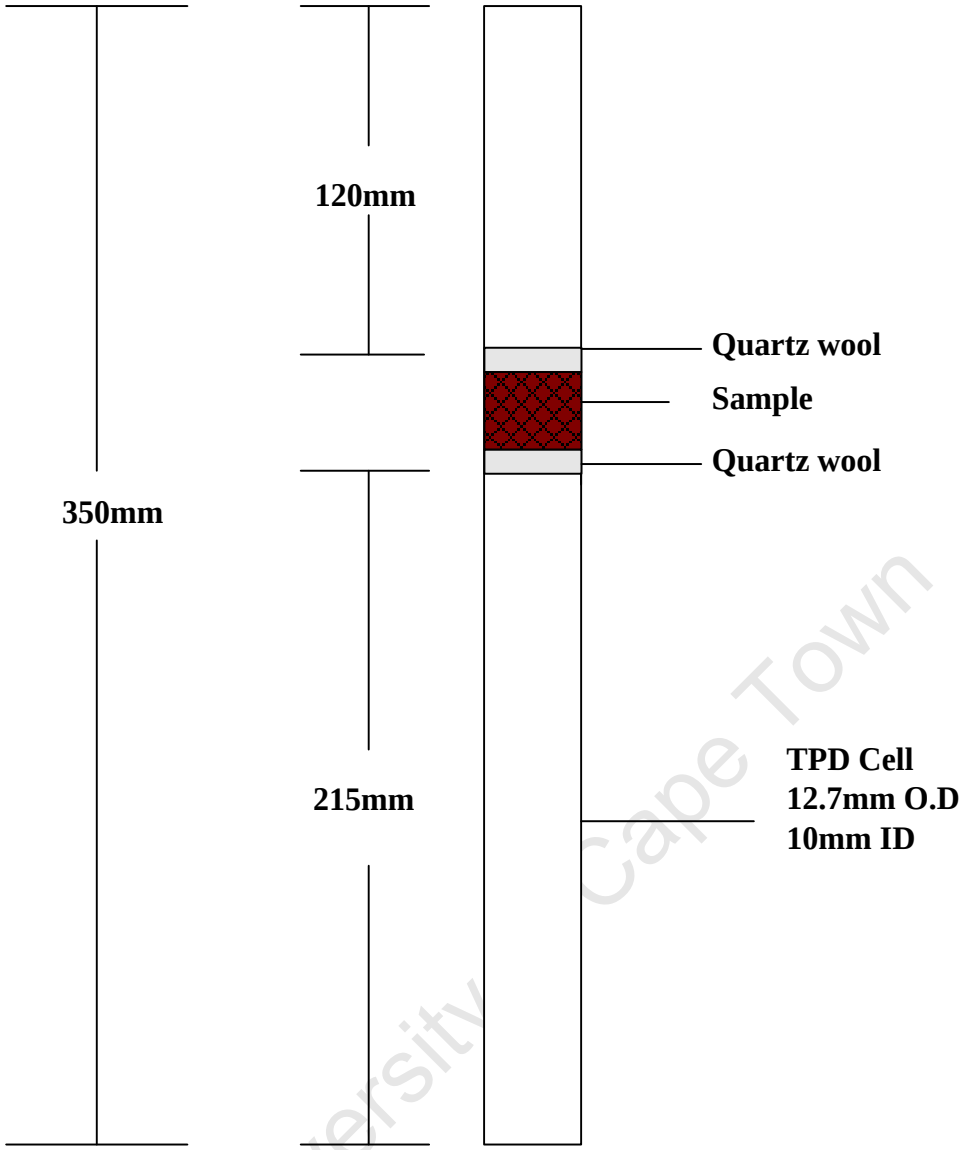

Figure 2.3: The TPD Cell

The temperature of the furnace is controlled using the temperature programmer, and the thermocouples are used to control and monitor the temperature thus ensuring that the temperature of the sample is accurately ramped.

The quantity of chemisorbed ammonia was recorded using a thermal conductivity detector (TCD) attached to a Hewlett Packard Vectra QS/16S computer. Eagle PC26 ISA bus was used for data capturing. The signal to be logged was connected to analogue channel CHO (input) on the PC26 card.

A typical TPD experiment consists of several steps:

- **Pre-treatment**

  The sample is first subjected in air for calcination (60ml (STP)/min/g; heating rate 10^{o}C/min) usually at elevated temperatures of 500^{o}C for 4-5 hours to remove impurities and to prepare the catalyst surface for the adsorption step.

- **Adsorption**

  The sample comes into contact with a molecule of interest (NH_3) in one of the several different modes; including pulse adsorption, steady flow adsorption, or static non-flow adsorption. The adsorption process may be carried out to the extent that the surface is fully covered with adsorption molecules. Amenomiya and Cvetanović (1969) proposed that if the activation energy and the peak maximum temperature is constant, then only the peak size would change depending on the amount of material adsorbed.

- **Desorption**

  After the surface has been in contact with the adsorbing molecule, for the purpose of achieving the desired coverage, the temperature of the system is raised in a linear fashion while a constant flow of an inert gas passes over a catalyst. Molecules leaving the catalyst surface are swept into the stream of inert gas and are carried to a detector, which monitors the amount of gas and the temperature at which it desorbs. Desorption into the gas stream occurs when an adsorbed species gains enough energy to over come the activation energy barrier to the desorption process [Weber; 1999].

2.2.3.1 Experimental Procedure

The catalyst (0.25g) was placed in a quartz cell by dispersing it evenly in the cell, a small piece of quartz wool was placed loosely onto and under the catalyst to allow good mixing of the gases and keep the catalyst in place. The reactor was then closed with a thermocouple positioned so that the temperature inside the catalyst bed can be measured. The heating mantle was placed around the cell with the thermocouple positioned between the cell and the heating mantle to measure the temperature at the wall of the cell. The catalyst was calcined at 500^{o}C for 4 hours with a flow rate of 60ml (STP)/min/g; heating rate 10^{o}C/min) in synthetic air before adsorption. Only the temperature inside the cell was recorded for measurements and not the wall temperature.

During the 4 hours of calcination, the detector was not switched on, thus calcination was not recorded, there after the detector was switched on. The catalyst was cooled down from 500^{o}C to 150°C and 1.17% NH_3 in He (60ml (STP)/min) was adsorbed at 150°C for 2 hours. After adsorption, the gas passing over the catalyst was changed from 1.17% NH_3 in He to helium. The catalyst was left under flowing He for 16 hours at 150^{o}C to remove physisorbed NH_3 this was not recorded, only 2 hours prior and 2 hours after the 16 hours of flushing was recorded. The furnace was further ramped up at 10^{o}C/min from the adsorption temperature (150^{o}C) to 600^{o}C in helium (60ml (STP)/min/g; heating rate 10^{o}C/min). The ammonia content was monitored using a TCD. The total amount of ammonia was quantified by back titration of 20ml 0.1N H_2SO_4 (Kimix) in 100ml distilled water and was trapped in 0.1N NaOH (Kimix) solution using bromothymol blue (Saarchem) as an indicator.

3 Results

3.1 Material Characterisation

3.1.1 Composition

Atomic absorption spectroscopy was used to obtain the potassium content in iron oxide as well as Si/Al content in H-ZSM-5 catalysts. The samples were digested as described in Chapter 2.2.1 and the concentration of the various compounds in the resulting solutions was determined on the spectrophotometer. The concentration value obtained from the analysis was converted into a mass-% by:

$$M(wt\%) = \frac{c}{m \times 100}$$

where:

c: concentration in mg/l (ppm) obtained from AAS

m mass of sample digested and made up to 100 ml solution for measurement

Determination of Fe and K content in iron based sample

The samples were prepared by digestion for the AAS-analysis. The finely prepared sample of precipitated and calcined iron oxide and the calcined sample impregnated with KNO_3 were dissolved in a mixture of hydrofluoric acid and perchloric acid. The samples were made to a known volume and filtered. The concentration of iron and potassium was determined using AA spectro-photometry. The iron and potassium content are shown in Table 3.1.

The iron content is compared to the content, if the iron in the sample is present as hematite. The iron content in the precipitated and calcined iron oxide sample corresponds to that in hematite. The potassium content corresponds well to the intended potassium loading assuming potassium to be present as KNO_3. Thus, the calcination in air at 350°C seems to be inefficient to transform potassium nitrate into K_2O.

Table 3.1: Metal content in calcined, precipitated iron oxide and iron oxide impregnated with potassium nitrate as determined using AAS

Sample		Iron oxide	KNO_3-impregnated sample
Fe-content, wt-%	measured	69.9	62.8
	expected	69.9[1]	62.9[2]
K-content, wt.-%	measured	-	4.0
	expected	-	3.9[2]

[1] Iron content expected if iron phase is hematite (Fe_2O_3)

[2] Iron content expected if iron phase is hematite (Fe_2O_3) and all potassium present as KNO_3

Determination of Al- and Na-content in H-ZSM-5

The supplied ZSM-5 sample has a SiO_2/Al_2O_3 ratio of 20. The sample was ion-exchanged in order to remove all Na^+-ions. Aluminium and sodium content of the sample was determined using AAS. For that purpose, the ion-exchanged sample of H-ZSM-5 was digested using hydrofluoric. The amount of Al as determined by AAS is shown in Table 3.2. The amount of sodium detected on H-ZSM-5 catalyst after NH_3 ion exchange ranged between 0 – 0.12mmol Na/g. This amount is small and complete (100%) ion-exchange can

be assumed. The aluminium content determined by AAS corresponded well with the expected calculated aluminium value.

Table 3.2: Aluminium content in ion-exchanged H-ZSM-5 (SiO_2/Al_2O_3 =20) as determined using AAS

Expected Al-content mmol/g	Si/Al mol/mol	SiO_2/Al_2O_3 mol/mol
0.4065	40	20

3.1.2 Catalyst Structure and Morphology

3.1.2.1 Iron oxide and potassium containing iron oxide

X-ray Diffraction (XRD)

The phase purity of the prepared calcined iron precipitate species were characterized using XRD. The prepared sample is defined as phase-pure if all the peaks in the XRD spectrum are attributable to a single phase. The presence of additional peaks indicates the presence of another phase in the sample.

Figure 3.1 shows the XRD patterns of an iron oxide sample prepared by precipitation followed by calcination in air at 350^{o}C. The XRD pattern of iron oxide shows intense peaks which are a characteristic of hematite (the standard reference pattern is given in appendix A).

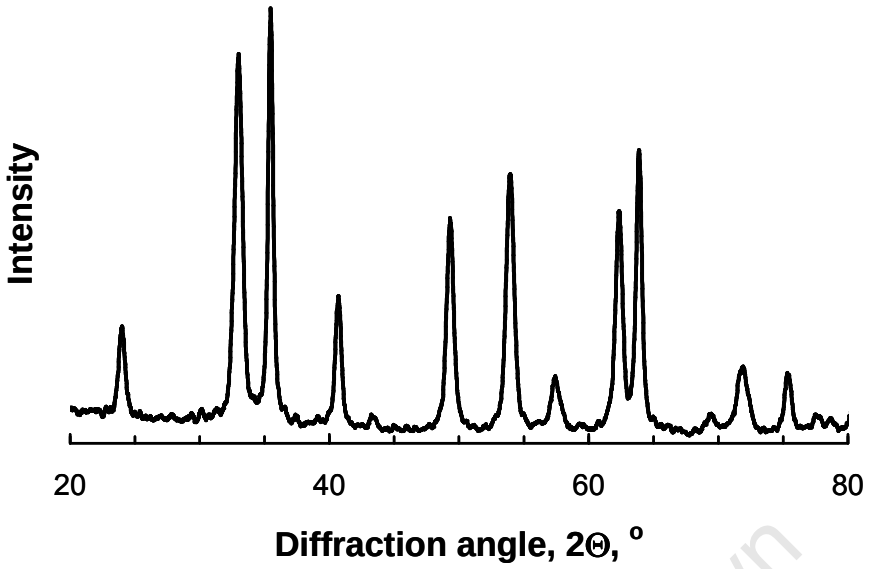

Figure 3.1: XRD pattern of iron oxide precipitate calcined for 8 hours in air (270ml (STP)/min/g) at 350°C (heating rate 10°C/min)

Hence, it can be concluded based on the XRD spectrum that the prepared sample is pure hematite (Fe_2O_3). The average crystallite size of the hematite phase within the samples was estimated using the Debye-Scherrer equation (see Table 3.3). The hematite phase has crystallites with an average diameter of ca. 38nm. The crystallite size is independent of the d-spacing and thus the diffraction plane implying approximately spherical crystallites.

Table 3.3: Average crystallite sizes of the hematite phase in the precipitated iron oxide sample (calcined for 8 hours in air - 270ml (STP)/min/g - at 350°C - heating rate 10°C/min) as determined by XRD-line broadening

Diffraction angle, 2θ, °	d-spacing, Å	$d_{crystal,}$ nm
24.2	3.68	37 ± 5
33.3	2.70	36 ± 4
35.5	2.51	43 ± 5
40.9	2.20	40 ± 3
49.5	1.83	37 ± 5
54.2	1.69	35 ± 4
57.7	1.59	34 ± 6
62.5	1.48	40 ± 4
64.1	1.45	43 ± 3
72.1	1.31	37 ± 5
75.7	1.26	37 ± 5

Figure 3.2 shows the XRD patterns of potassium promoted iron oxide sample prepared by precipitation, calcination and subsequent impregnation with KNO_3 (6.7g K_2O/100g Fe). The XRD pattern of K-Fe_2O_3 shows intense peaks similar to those of the unpromoted precipitated iron oxide, which are thus attributable to hematite.

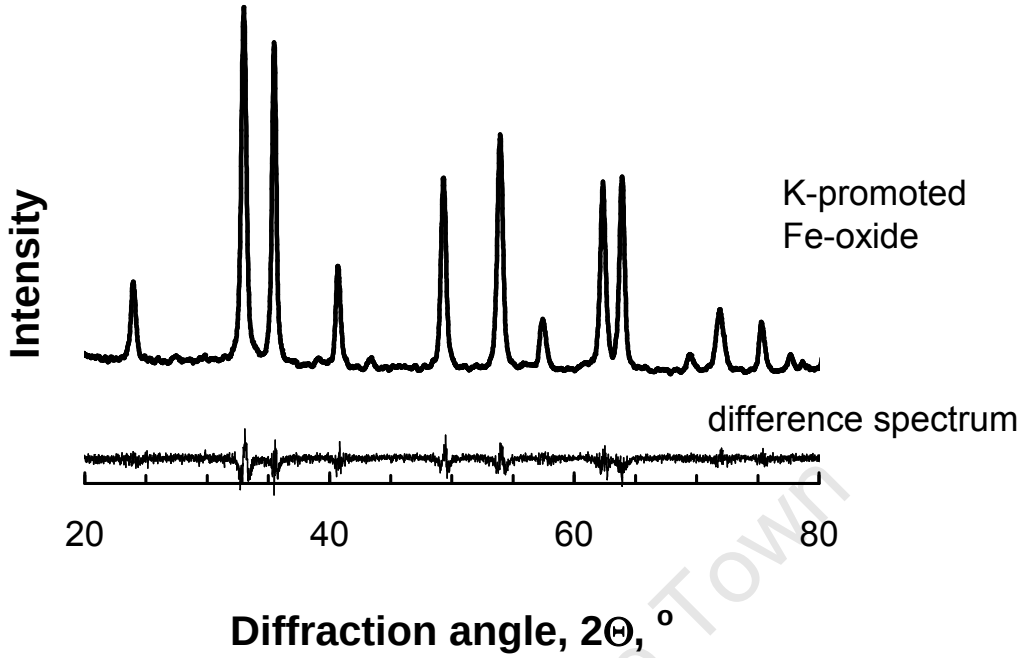

Figure 3.2: XRD pattern of precipitated and calcined iron oxide sample after impregnation with KNO_3 and subsequent calcination and the difference between the XRD pattern of the potassium impregnated sample and the original sample.

Thus the addition of potassium to the sample does not influence the iron oxide crystal phases present in the sample (after impregnation with KNO_3 and subsequent calcination) and does not give rise to a crystalline phase containing potassium. This is further evidenced by the lack of additional diffraction peaks in the difference spectrum (taken as the difference between the XRD-spectrum of the precipitated and calcined iron oxide and the XRD-spectrum of the subsequent KNO_3-impregnated and calcined sample). The slight shift in the diffraction angles might be attributed to instrumental error.

The average crystallite size of the hematite phase present in the sample does not change upon impregnating the calcined iron oxide precipitate with KNO_3 (see Table 3.4). It can thus be concluded that impregnation of the calcined, precipitated iron oxide with KNO_3 and subsequent calcination at 350^{o}C in air for 8 hours does not affect the morphology of the hematite crystallites present in the sample.

Table 3.4: Average crystallite sizes of the hematite phase in the precipitated iron oxide sample (calcined for 8 hours in air - 270ml (STP)/min/g - at 350^{o}C - heating rate 10^{o}C/min) impregnated with KNO_3 (6.7g K_2O/100g Fe) and re-calcined in air for 8 hours at 350^{o}C as determined by XRD-line broadening

Diffraction angle, 2θ, ^{o}	d-spacing, Å	$d_{crystal,}$ nm
24.03	3.70	34 $\pm$ 6
33.03	2.71	36 $\pm$ 4
35.45	2.53	43 $\pm$ 5
40.79	2.21	41 $\pm$ 2
49.2	1.85	38 $\pm$ 4
53.9	1.70	36 $\pm$ 4
57.17	1.61	35 $\pm$ 6
62.3	1.49	40 $\pm$ 4
63.7	1.46	44 $\pm$ 5
71.4	1.32	38 $\pm$ 4
74.67	1.27	36 $\pm$ 5

Scanning Electron Microscopy (SEM)

The SEM photograph of calcined iron oxide (Fe_2O_3) prepared by precipitation is shown in figure 3.3. The material consists of particles with a large variation in sizes (in the range of a few to approximately 100 μm). Each of these particles will consist of a large number of crystallites.

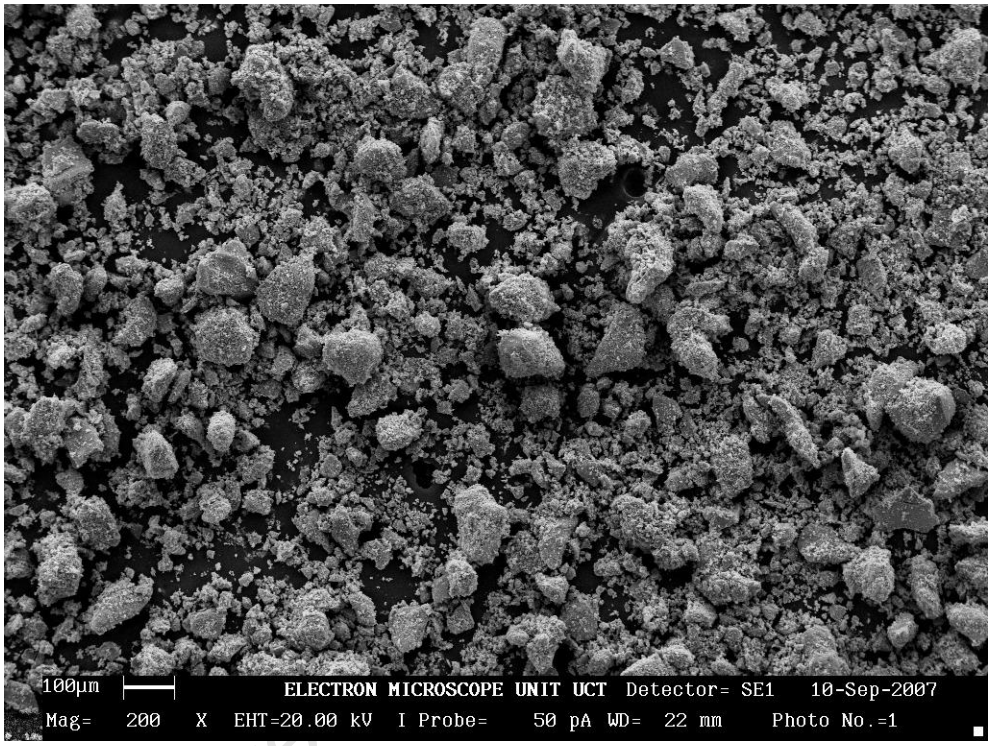

Figure 3.3: Scanning Electron Microscopy image of iron oxide precipitate calcined for 8 hours in air (270ml (STP)/min/g) at 350^{o}C (heating rate 10^{o}C/min)

3.1.2.2 H-ZSM-5

X-ray Diffraction (XRD)

Figure 3.4 shows the XRD pattern of ion exchanged H-ZSM-5 sample (the standard reference pattern is given in appendix A). It can be seen from the XRD pattern that this sample is both highly crystalline and has high phase purity. The phase appears to be pure, since all the peaks are attributable to H-ZSM-5, thus it can be said that ion exchange was complete and the sample is phase pure

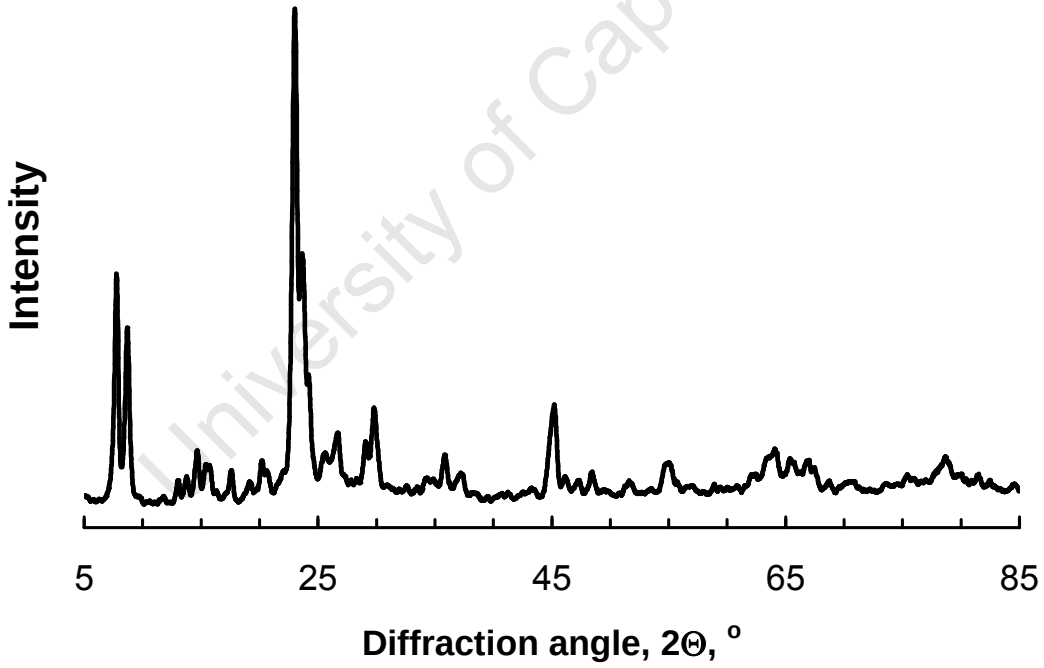

Figure 3.4: XRD pattern of H-ZSM-5 after ion-exchange

The average crystallite size was estimated by line broadening analysis (see Table 3.5), using the Debye-Scherrer equation. The crystallite size of H-ZSM-5, taking into accounts the error in the measurement to approximate the crystallite diameter to about 52nm from the measured peaks.

Table 3.5: Crystallite sizes of H-ZSM-5 after ion-exchange as determined by XRD-line broadening

Diffraction angle, 2θ, °	d-spacing, Å	$d_{crystal,}$ nm
7.9	11.1	47 ± 10
8.8	10.0	48 ± 7
23.9	3.71	58 ± 6
24.3	3.65	52 ± 9
24.7	3.59	49 ± 11

Scanning Electron Microscope (SEM)

The SEM photograph of calcined H-ZSM-5 which was ion exchanged for the purpose of removing all the Na^+-ions present is shown in Figure 3.5. The catalyst consists of a variation and irregularity in particle sizes. The material consists of particles of various sizes probably due to synthesis conditions.

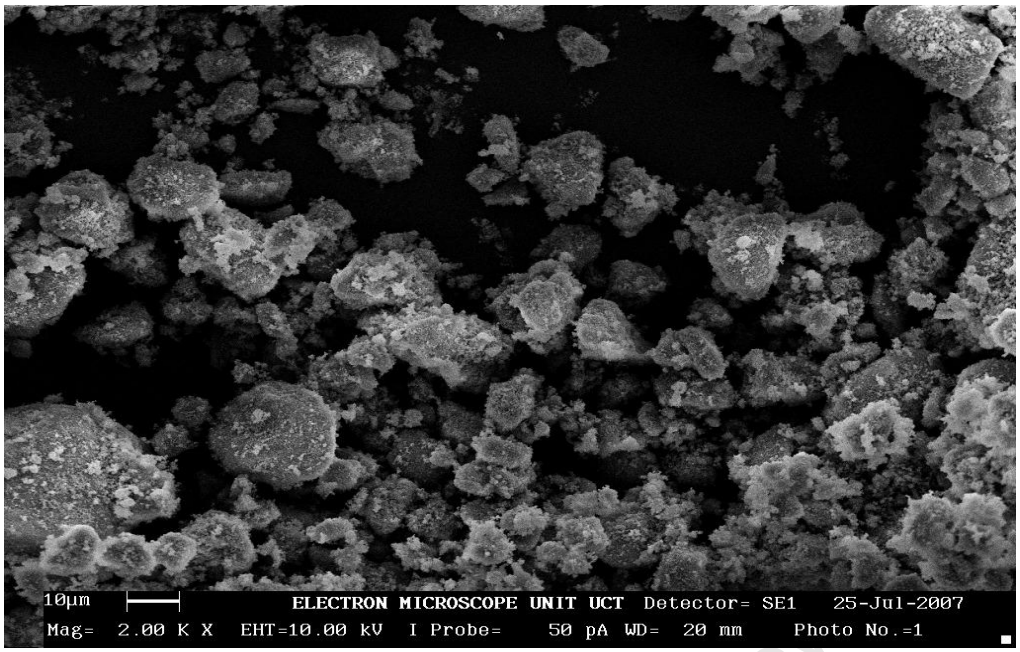

Figure 3.5: Scanning Electron Microscopy image of calcined and ion-exchanged H-ZSM-5

NH_3-Temperature Programmed Desorption (NH_3-TPD) over H-ZSM-5

Temperature programmed desorption of ammonia is a well described technique to characterize acidity in heterogeneous catalysts [Lowenthal et al., 1995; Rajagopal et al., 1995; Ma et al., 2004]. The original ion exchanged H-ZSM-5 was characterized using NH_3-TPD, to measure the number of acid sites. Figure 3.6 shows the events in the NH_3-TPD experiment as a function of time and the resulting desorption spectrum of the parent HZSM-5. After calcination of the sample in air, it was cooled down to 150^{o}C in He.

Subsequently, ammonia was adsorbed from a stream containing 1.17% NH_3 in He. Weakly adsorbed ammonia was removed isothermally by flushing with helium for ca. 2 hours. Subsequently, temperature was raised and the amount of ammonia desorbed was determined.

The parent H-ZSM-5 showed a maximum in the rate of ammonia desorption at 350^{o}C. A single peak in ammonia-TPD of H-ZSM-5 is usually observed, and a peak maximum at ca. 350^{o}C has been reported before for H-ZSM-5 with Si/Al=36 (Weber *et al.*, 1996).

The number of acid sites obtained for H-ZSM-5 by integration of the TPD-spectrum was 0.4065 mmol NH_3 per gram of catalyst which corresponds well with the value by back titration (0.4 mmol/g; see Table 3.6). The amount of NH_3 desorbed as determined by integration of the TPD-signal corresponds to a Si/Al-ratio in the zeolite of 40 assuming that all aluminium is associated with acid sites.

Table 3.6: Analysis of NH_3-TPD of ion-exchanged H-ZSM-5 sample

Catalyst	NH_3-TPD (mmol/g) integration of TCD signal	NH_3-TPD (mmol/g) titration	T_{max} ^{o}C
H-ZSM-5	0.4065	0.40	368

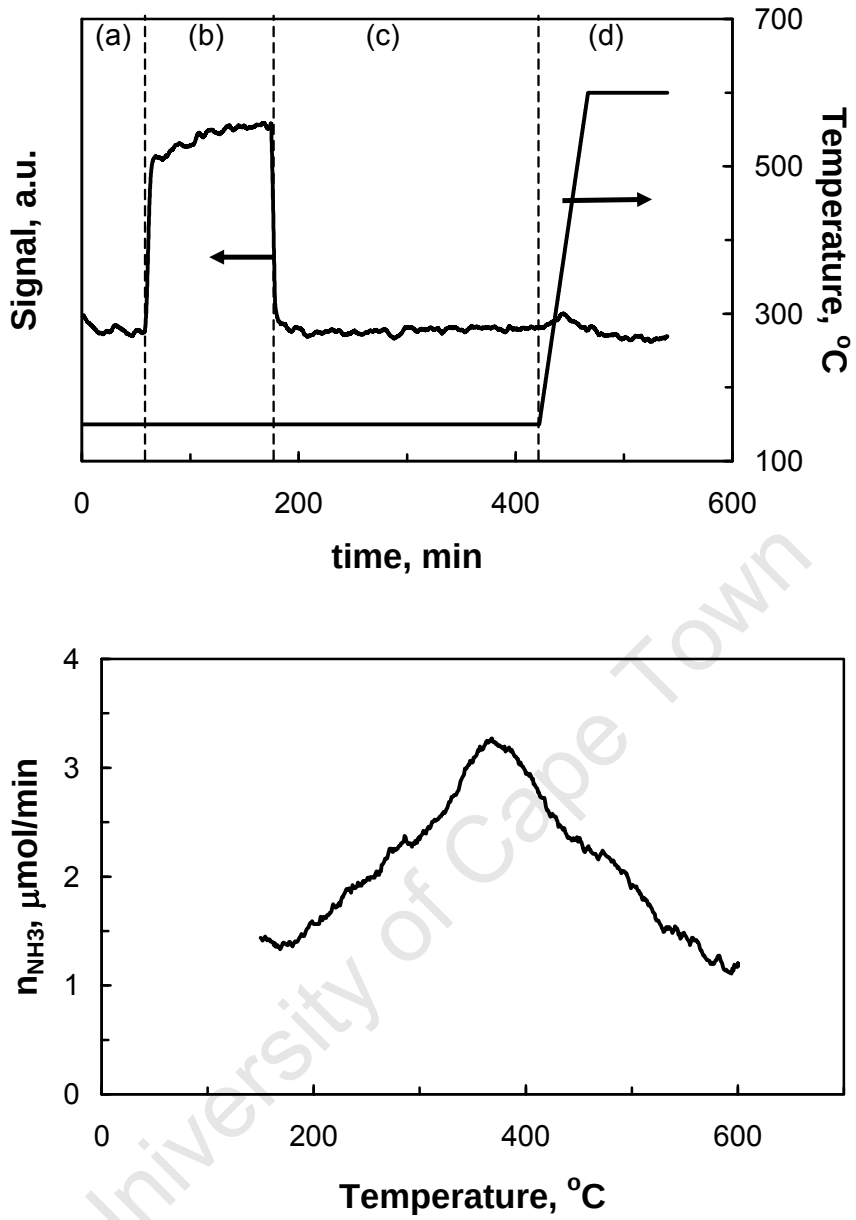

Figure 3.6: Ammonia TPD on calcined and ion-exchanged H-ZSM-5

Top: Events during ammonia TPD after calcination of sample in air at 500°C for 5 hours

(a): flushing in He at 150°C

(b): adsorption of ammonia from 1.17% NH_3 in He stream at 150°C

(c): flushing in He at 150°C

(d): temperature programmed desorption of ammonia

Bottom: NH_3-TPD spectrum of zeolite H-ZSM-5 (mass of zeolite: 250 mg)

The total amount of ammonia was quantified by back titration of sulphuric acid trapped in sodium hydroxide. This was only done for the original sample of H-ZSM-5, because the rest of the samples results were quantified by other techniques including EDX. In order to have reproducible values by titration technique, variables such as titration time, volume of added indicator, pore size and moisture should be carefully considered.

Even in cases when all experimental precautions have been taken, titration method suffers from a number of limitations, which include the fact that equilibrium is rarely achieved, thus the acidity data from the indicator method should not be used straight forward to predict catalytic behaviour. Another problem which can arise from titration is visual determination of the colour change which is subjective when a coloured or dark catalyst sample is used [Corma, 1995]. Thus it was better to quantify one sample by titration and the rest by other techniques.

3.2 Diffusion of potassium on K-Fe_2O_3/H-ZSM-5 pellets

The iron oxide sample impregnated with KNO_3 and the H-ZSM-5 powder was pressed into a layered pellet (as described in Chapter 2.1.3). The pellets were heated to 350^{o}C in an oven for a certain time. The integrity of the phases and the potassium distribution over the pellet was determined after heating.

3.2.1 X-Ray diffraction

The combined pellets containing H-ZSM-5 and K-Fe_2O_3 were heated at 350^{o}C for a number of days after which were separated and crushed into powder

samples. The iron oxide sample that was obtained after separating the pellet was characterized by XRD to determine a change in crystallite size (see Figure 3.7). The result obtained from 1, 3 and 6 days of heating showed that, the average crystallite size does not change. Thus it can be concluded that prolonged heating at 350^{o}C does not affect the average crystallite size of the hematite phase present in the sample.

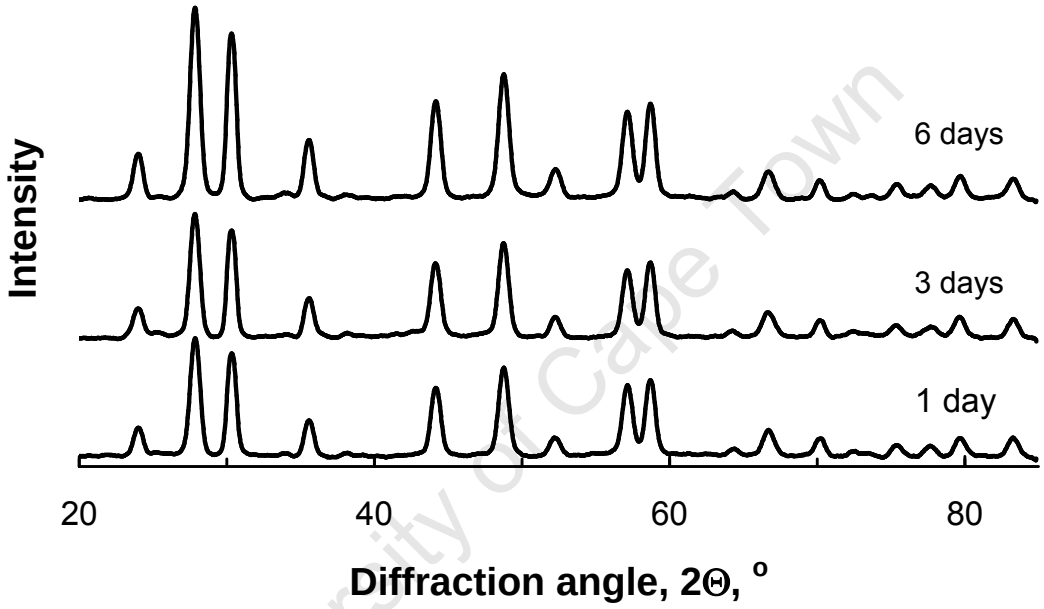

Figure 3.7: XRD pattern of K-Fe_2O_3 sample obtained from separation of K-Fe_2O_3/H-ZSM-5 pellets after heating at 350^{o}C for various times

Table 3.7: Crystallite sizes of K-Fe_2O_3 sample obtained from separation of K-Fe_2O_3/H-ZSM-5 pellets after heating at 350°C for various times

Diffraction angle, 2θ, °	1 Day $d_{crystal}$, nm	3 Days $d_{crystal}$, nm	6 Days $d_{crystal}$, nm
27.94	33 ± 5	34 ± 6	33 ± 4
30.42	37 ± 4	35 ± 5	38 ± 4
35.45	43 ± 5	41 ± 5	40 ± 5
35.70	40 ± 2	38 ± 4	43 ± 4
44.28	40 ± 4	40 ± 2	41± 2
48.88	36 ± 4	37 ± 5	36 ± 4
52.46	34 ± 6	35 ± 6	38 ± 2
57.27	40 ± 4	39 ± 5	43 ± 4
58.84	42 ± 5	44 ± 5	40 ± 5
66.95	35 ± 4	37 ± 4	38 ± 4
70.45	36 ± 5	34 ± 4	33± 5

3.2.2 Energy Dispersion X-ray Spectrometer (EDX)

EDX was used to monitor the concentration profile of iron, potassium, silicon, aluminium as a function of the position in the pellet and time of heating at 350°C. The analysis was performed with E = 10-20 kV i.e 0.01-0.02 MeV, this results in a penetration depth of ca 0.5-2μm. When an electron passes through a sample there are two main types of interactions:

1. Elastic scattering: where the electron changes direction with negligible loss of energy.
2. Inelastic scattering: where the electron loses energy, but usually has a negligible change of direction.

The depth of penetration for X-ray excitation depends on the particular X-ray line. The X-ray signal depends on the diameter of the beam, the diffusion of the electron in the sample and on the critical excitation energies.

The diameter of the X-ray distribution can be derived approximately from the depth of penetration. The electron intensity generated by the electron bombardment of the sample depends on the number of factors – the atomic number, the particular electron shell, the efficiency of the X-ray detected.

Particles size range between 78 - 114μm. Thus the electron bundle will not penetrate the sample because electrons can penetrate up to 2μm of the sample. This may lead to an under estimation of concentrations.

3.2.2.1 EDX profile for pellet containing H-ZSM-5 and Fe_2O_3

Before potassium diffusion could be investigated, an investigation on the mobility of Fe, Si and Al was conducted using a pellet containing unpromoted iron oxide and H-ZSM-5. The pellet was heated at 350^{o}C for 96 hours to check whether Fe, Al or Si was diffusing (see Figure 3.8). It was shown that in the limited time none of the components were diffusing.

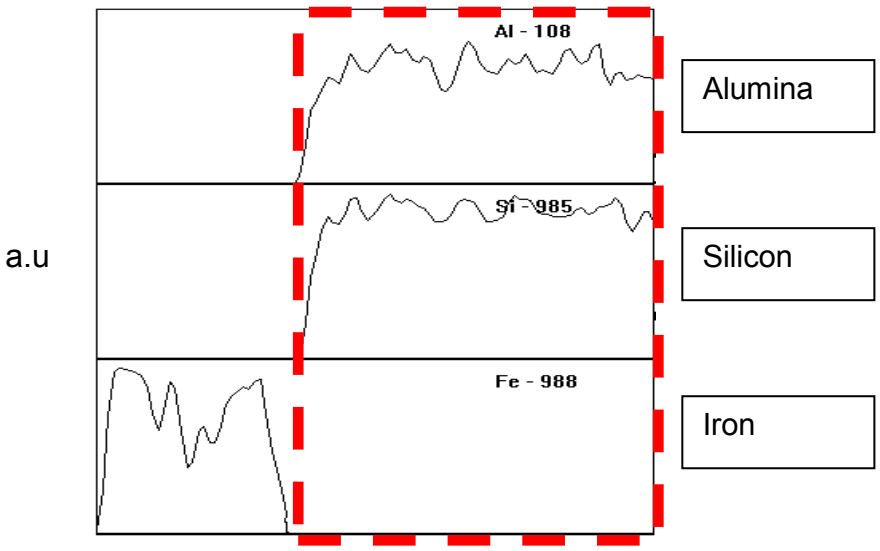

Figure 3.8: EDX profile for a pellet containing H-ZSM-5 and Fe_2O_3 after being exposed to temperatures of 350^{o}C for 96 hours

3.2.2.2 EDX profile for pellet containing K-Fe_2O_3 and Fe_2O_3

Figures 3.9 shows how EDX can be used to determine potassium migration as a function of position in a pellet and time on stream. The concentration profile of potassium in a pellet consisting of unpromoted Fe_2O_3 and K/Fe_2O_3 clearly shows the region of the pellet consisting of K/Fe_2O_3 and the region poor in potassium (highlighted in red in Figure 3.9) containing the unpromoted Fe_2O_3. A flat profile for K and Fe is obtained after heating the combined pellet at 350^{o}C for 6 days. The average K/Fe ratio (in arbitrary units) was 0.35±0.04. Thus, potassium migration on Fe_2O_3 is relatively fast and after 6 days potassium was uniformly distributed over the pellet.

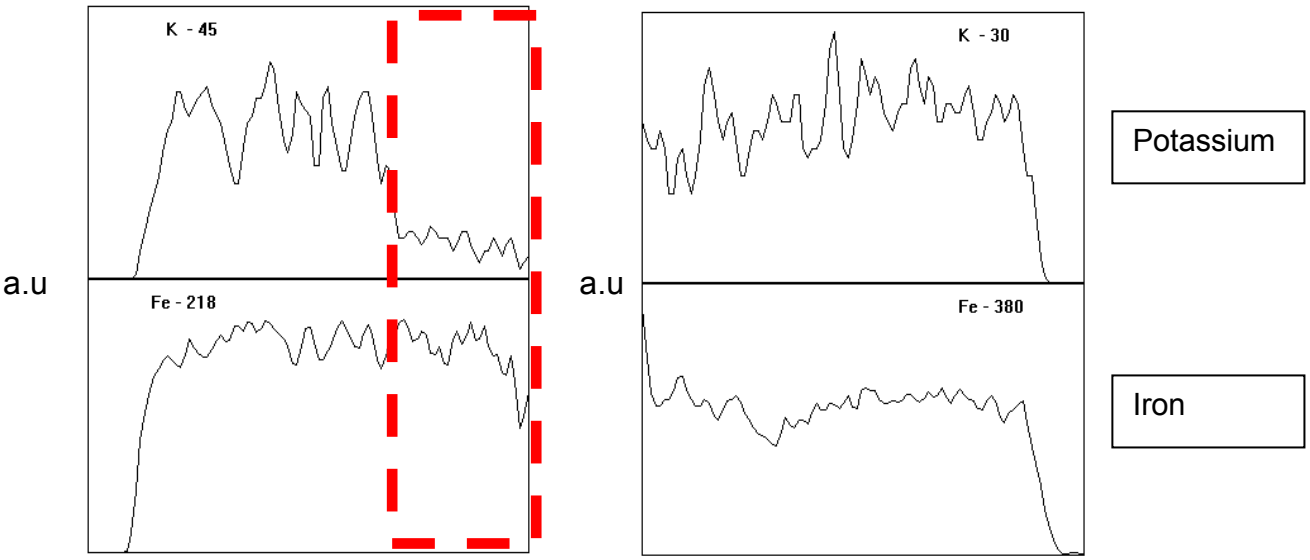

Figure 3.9: EDX profile for a pellet containing K/Fe_2O_3 and Fe_2O_3
left: untreated pellet
right: pellet heated at 350°C for 6 days

3.2.2.3 EDX profile for a pellet containing K/Fe_2O_3 and H-ZSM-5

Figure 3.10 shows the obtained EDX-profiles of K, Fe, Si and Al for various heating times. A rather sharp decrease in the Fe-concentration and a sharp increase in the Al- and Si-concentration are observed in the EDX-profiles at the interface between these parts of the pellet. This boundary is typically located at a relative length of 0.3, since the pellets were synthesized using equal mass of Fe_2O_3 and H-ZSM-5. The difference in the density between these compounds will thus result in a much smaller zone containing Fe_2O_3 than the zone containing H-ZSM-5. Figure 3.11 shows the average Fe, K, Si and Al-concentration relative to the concentration of Fe, K, Si and Al along the cross-section of the pellet as determined by the line scan, which was determined by: $\overline{C_i} = \frac{\int_{cross-section} C_i(z) \cdot dz}{\ell_{cross-section}}$.

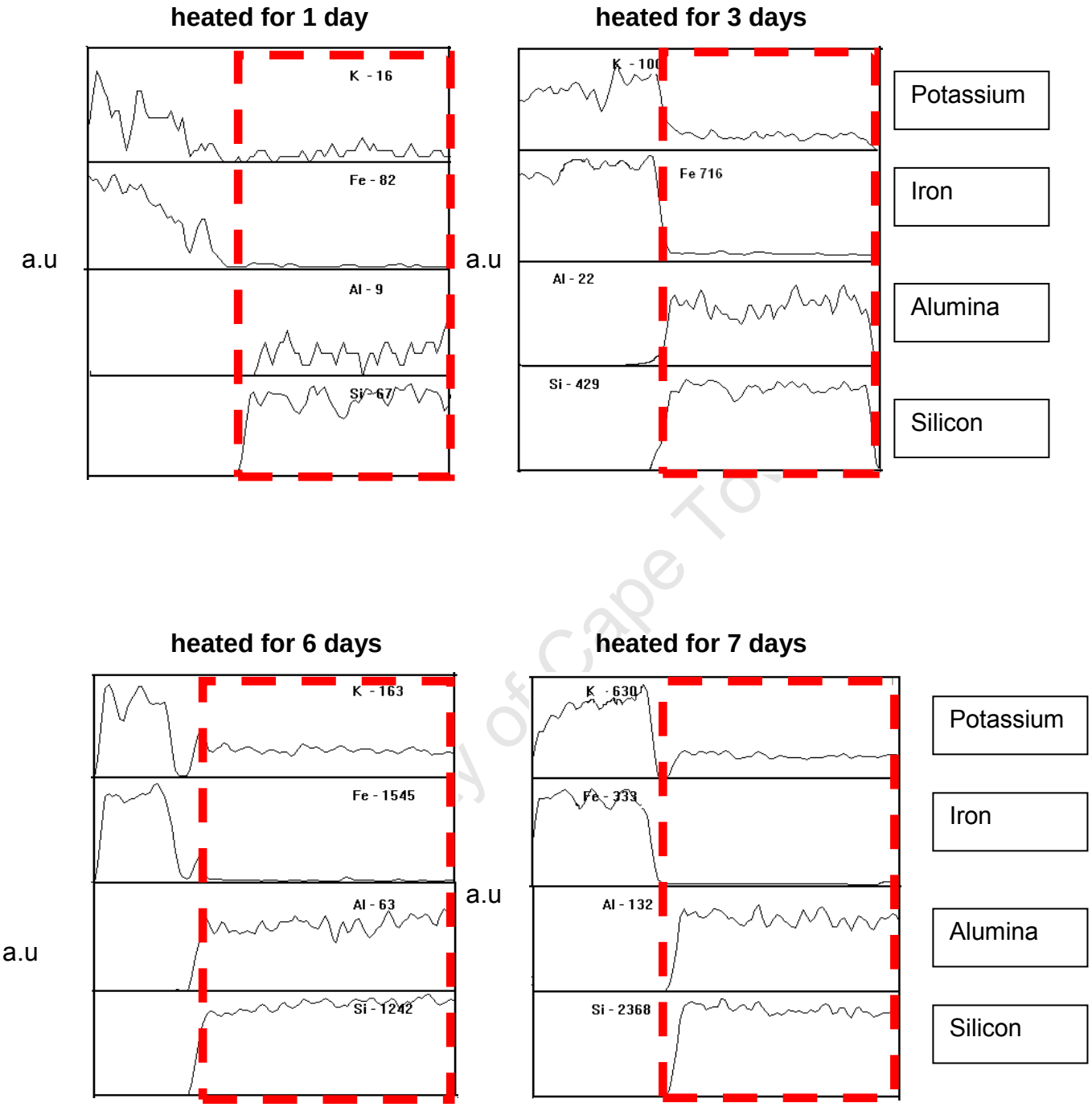

Figure 3.10: EDX analysis of pellets containing K-Fe2O3 and H-ZSM-5 heated at 350oC as a function of length of pellet (Numbers in the graph corresponds to the highest amount of a compound detected).

The average concentration of the various elements shows a large degree of scatter. It can be noted that in particular the samples heated for 2, 5 and 7 days at 350°C show a much higher Si-content and as a consequence a much lower Fe-content. EDX technique can in principle be used for qualitative and quantitative analysis. A single line-scan can yield more information with more statistical relevance gathered in a much shorter time, compared with X-ray mapping and point analysis [Griffin and Nockolds, 1990]. Matrix effects may how ever occur. Furthermore, sample inhomogeneity along the line-scan (e.g. unevenness along the line scan in the order of the penetration depth of the electron bundle) may affect the obtained concentration.

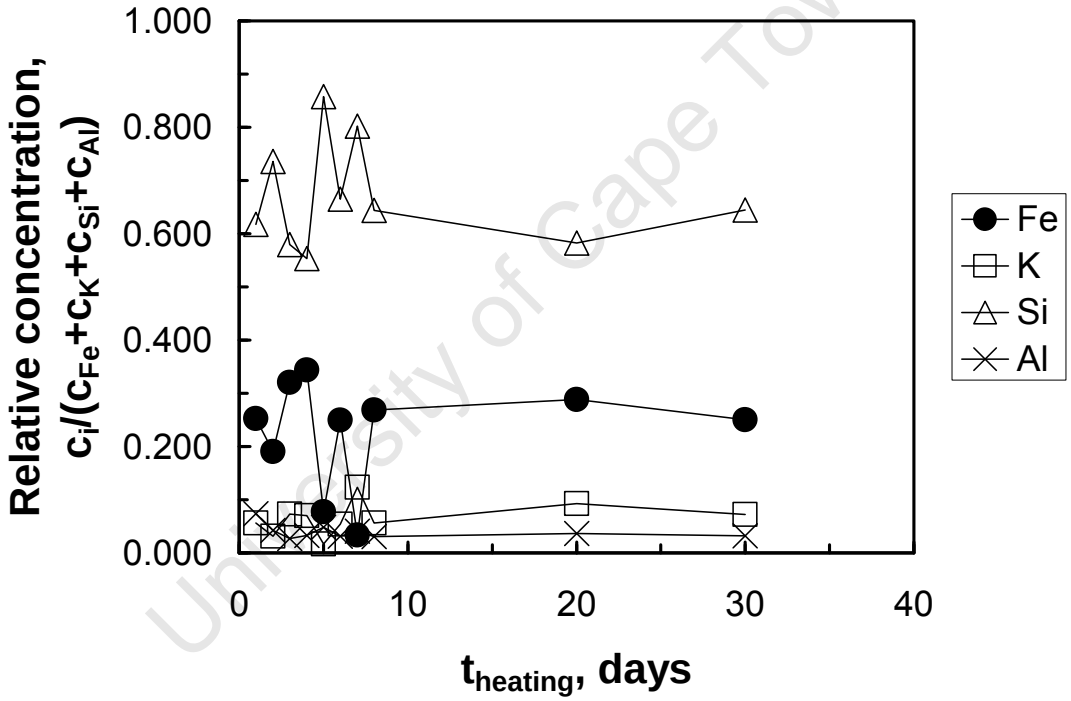

Figure 3.11: Normalized average concentration of Fe, K, Si and Al as a function of heating time at 350°C

Figure 3.12 shows the relative Fe-concentration in the pellet as a function of the relative position across the cross-sectional area of the pellet. The relative concentration of Fe was determined from the absolute value given by EDX

and scaling the obtained curves with respect to the maximum value obtained. The absolute Fe-concentration was taken relative to the absolute amount of iron and the absolute amount of silicon at any point across the cross-sectional area. It can be clearly seen that a sharp boundary exists between the zone originally containing the K-Fe_2O_3 and the zone originally containing H-ZSM-5.

The position of the boundary is not at exactly the same position and varies between z/L_{pellet} = 0.25-0.35 with an average of 0.30±0.03. The position of the phase boundary was expected to be at a relative position of z/L_{pellet} = 0.26, since the specific volume of Fe_2O_3 crystals is 0.19 cm^3/g and the specific volume of H-ZSM-5 crystals is 0.56 cm^3/g (based on 17.9 T-atoms/1000 $Å^3$). The difference might be attributed to differences in the pellet porosity in the zone containing originally K-Fe_2O_3 and the zone originally containing H-ZSM-5.

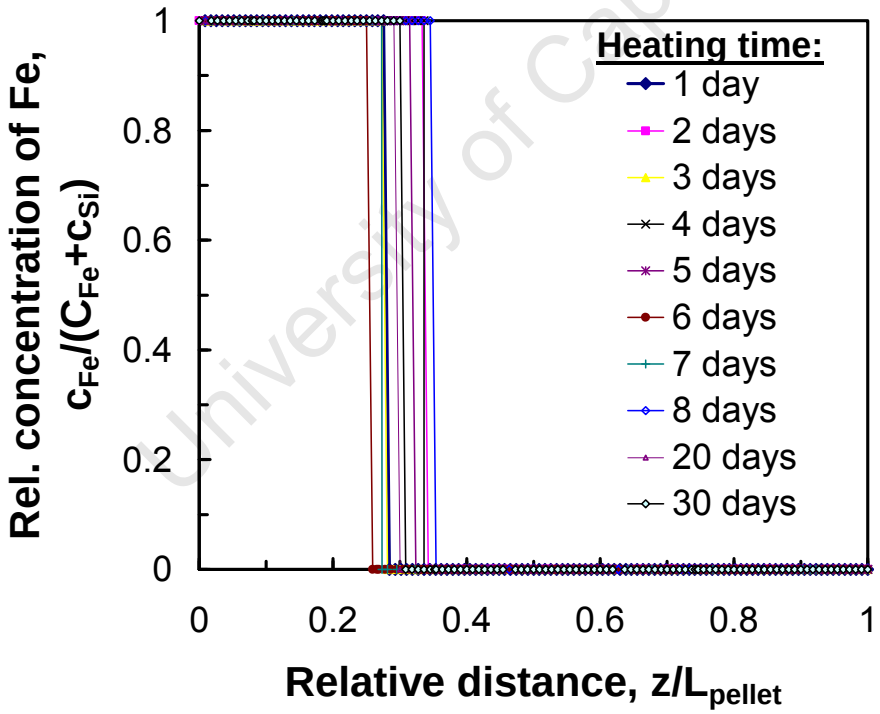

Figure 3.12: Normalized concentration profile of Fe relative to Fe and Si as a function of relative length of pellet after various times of heating at 350°C

This variation in the position of the phase boundary within the pellet originates from slight inhomogeneities on the surface of the pressed H-ZSM-5 pellet on top of which the K-Fe_2O_3 phase is pressed. The variation is quite large and must be taken into account when evaluating diffusivity of potassium.

A given cross-section of the pellet contains different amounts of the zone originally containing K-Fe_2O_3-phase and the zone originally containing the H-ZSM-5, although the pellet itself contains equal mass amounts of K-Fe_2O_3 and H-ZSM-5. Hence, the relative length of the pellet was normalized to ensure that the phase boundary was at $z/L_{pellet} = 0.3$:
for

$$\frac{z}{L_{pellet}} \leq 0.3 \qquad \left(\frac{z}{L_{pellet}}\right)_{normalized} = 0.3 \cdot \frac{\frac{z}{L_{pellet}}}{\left(\frac{z}{L_{pellet}}\right)_{boundary}}$$

$$\frac{z}{L_{pellet}} > 0.3 \qquad \left(\frac{z}{L_{pellet}}\right)_{normalized} = 0.3 + 0.7 \cdot \frac{\frac{z}{L_{pellet}} - \left(\frac{z}{L_{pellet}}\right)_{boundary}}{1 - \left(\frac{z}{L_{pellet}}\right)_{boundary}}$$

Figure 3.13 shows the Al-concentration relative to the amount of iron and silicon as a function of the normalized relative length in the pellet. The transition between the zone, which originally contained K-Fe_2O_3, and the zone, which originally contained H-ZSM-5 are now positioned at the same point. It can be further noted that the average concentration of Al in the zone, which originally contained H-ZSM-5, is approximately independent of the heating time, since all curves (with exception of the curve for 1 day of heating time) coincide. However, the variation in the relative content is rather large (ca. 10-15%).

The Al-concentration on the phase boundary seems to be enhanced. This is an artifact, since the concentration of aluminium and silicon differ substantially in the sample. The Al-concentration was recorded at a higher sensitivity, and is thus easier to pick the increase in the Al-content around the phase boundary in the pellet than the increase in the Si-content.

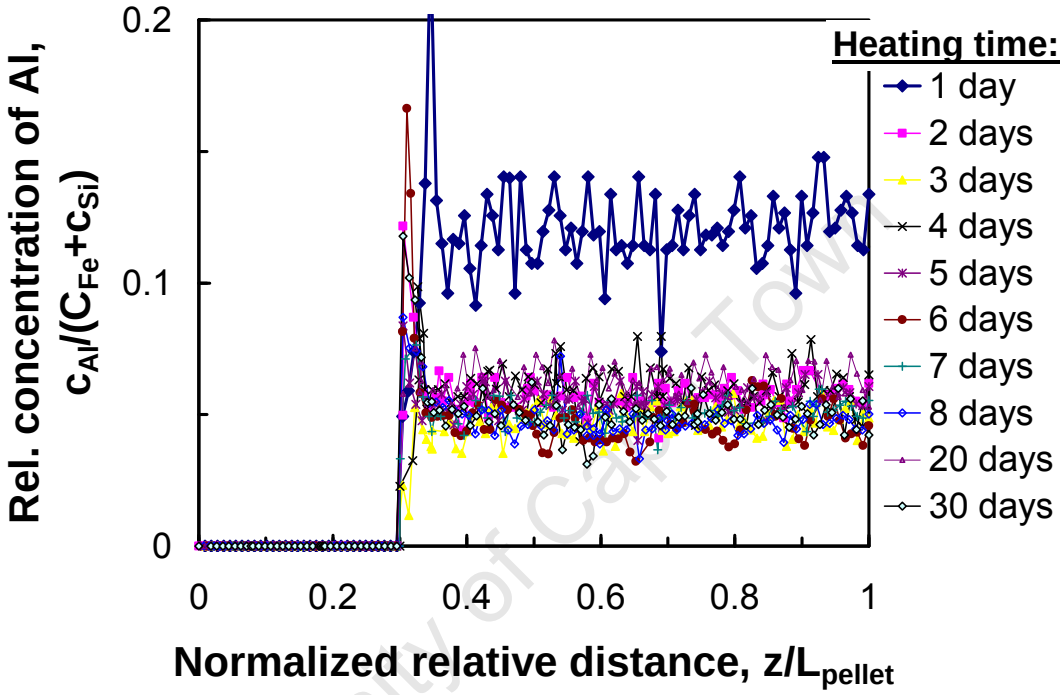

Figure 3.13: Normalized concentration profile of Al relative to Fe and Si as a function of normalized relative length of pellet after various times of heating at 350°C (length of pellet normalized relative to a fixed boundary between the zone, which originally contains K-Fe_2O_3, and the zone, which originally contains H-ZSM-5, at z/L_{pellet} = 0.3)

Figure 3.14 shows the amount of potassium relative to the amount of iron and silicon as a function of the normalized relative distance. A large scatter is observed in the relative potassium concentration. Despite the relative large

scatter, a strong concentration gradient can be observed across the phase boundary layer. A gradual change in the potassium level in both sections was expected, if diffusion of potassium on Fe_2O_3 and/or on H-ZSM-5 would control the migration of potassium. This is not observed (see also Figure 3.10). Hence, it must be concluded that the transport of potassium from the zone, which originally contained K-Fe_2O_3, to the zone, which originally contained H-ZSM-5, in a pellet pressed with a pressure of 2 tons is controlled by mass transfer over the boundary layer. The diffusion in a particular phase is relatively fast.

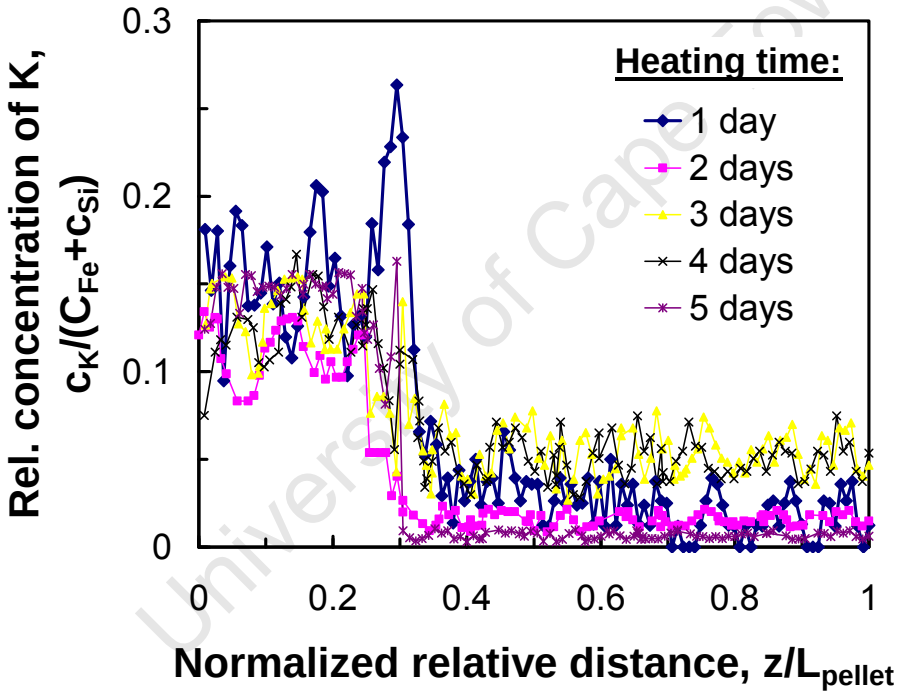

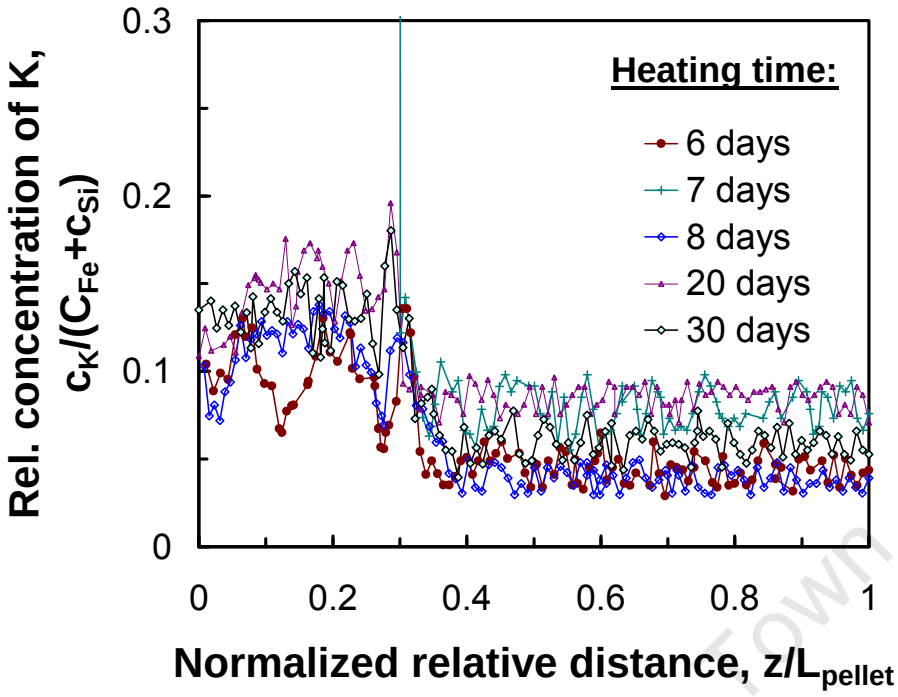

Figure 3.14: Normalized concentration profile of K relative to Fe and Si as a function of normalized relative length of pellet after various times of heating at 350°C (length of pellet normalized relative to a fixed boundary between the zone, which originally contains K-Fe_2O_3, and the zone, which originally contains H-ZSM-5, at z/L_{pellet} = 0.3)

The distribution of potassium in the various samples further shows that the total amount of potassium determined along the cross-section varies strongly from sample to sample (the potassium content for the sample heated for 7 days in the zone, which originally contained K-Fe_2O_3, is even off the scale of figure 3.14). Hence, the average potassium content in the zone, which originally contained K-Fe_2O_3, was normalized with respect to total amount of potassium along the cross-section.

$$f_{K,K-Fe_2O_3-zone} = \frac{\int_{K-Fe_2O_3-zone} C_K(z)\cdot dz}{\int_{total} C_K(z)\cdot dz}$$

Figure 3.15 shows the average potassium content in the zone, which originally contained K-Fe_2O_3, as a function of the heating time. The average potassium content in the zone originally containing K-Fe_2O_3 drops fast with heating time and seems to approach a constant value of ca. 0.45 after 7-30 days implying some equilibrium of the potassium in the zone originally containing K-Fe_2O_3 and the potassium in the zone originally containing H-ZSM-5.

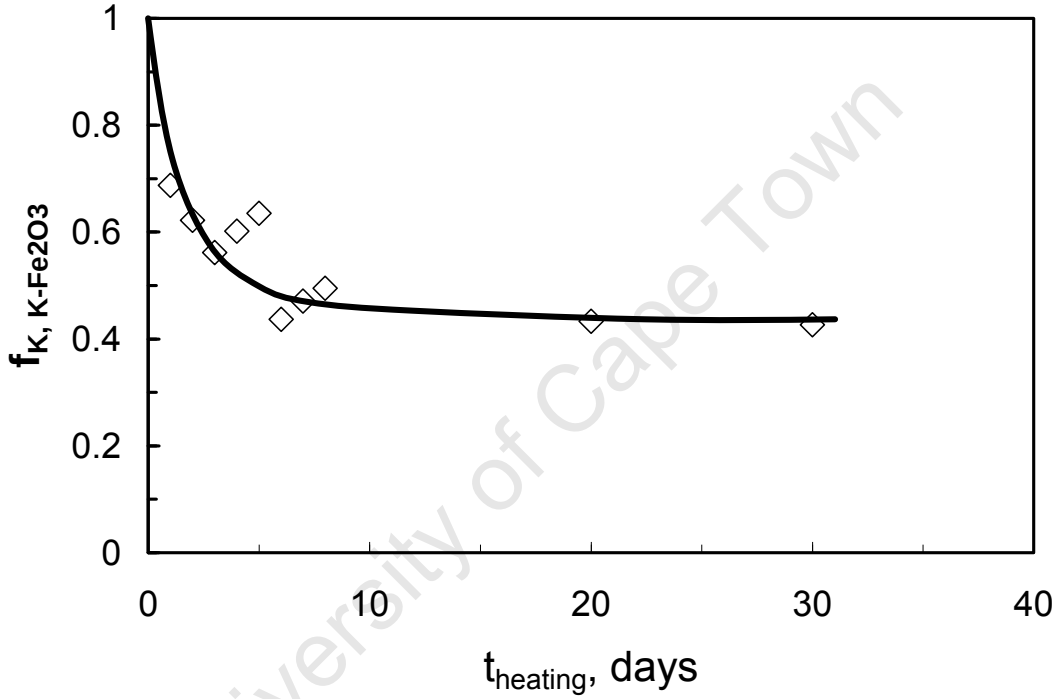

Figure 3.15: Fraction of potassium in the zone originally containing K-Fe_2O_3 relative to total amount of potassium along cross-section as a function of heating time at 350^{o}C

3.2.3 NH_3 - Temperature Programmed Desorption

The flat EDX-profile of the concentration of potassium in the zone originally containing H-ZSM-5 shows that potassium is equally distributed over ZSM-5. Potassium on ZSM-5 will ion-exchange with the protons present resulting in a decrease in the number of acid sites present in ZSM-5. The decrease in the number of acid sites can be monitored using e.g. NH_3-TPD. Temperature programmed desorption of pre-adsorbed ammonia from the surface of ZSM-5 was performed for the purpose of determining the number of acid sites as a function of heating time.

Combined pellets containing H-ZSM-5 and K/Fe_2O_3 were heated at 350^oC for a number of days after which were separated into its components. Each zone was crushed into powder samples and 0.25 g of the zeolite containing zone was characterized by NH_3-TPD. Figure 3.16 shows the NH_3-TPD-spectrum from H-ZSM-5 as a function of the heating time. With increasing heating time the temperature, at which the rate of desorption of ammonia is the highest, decreases. The amount of acid sites will decrease with increasing heating time due to migration of potassium to the zeolite.

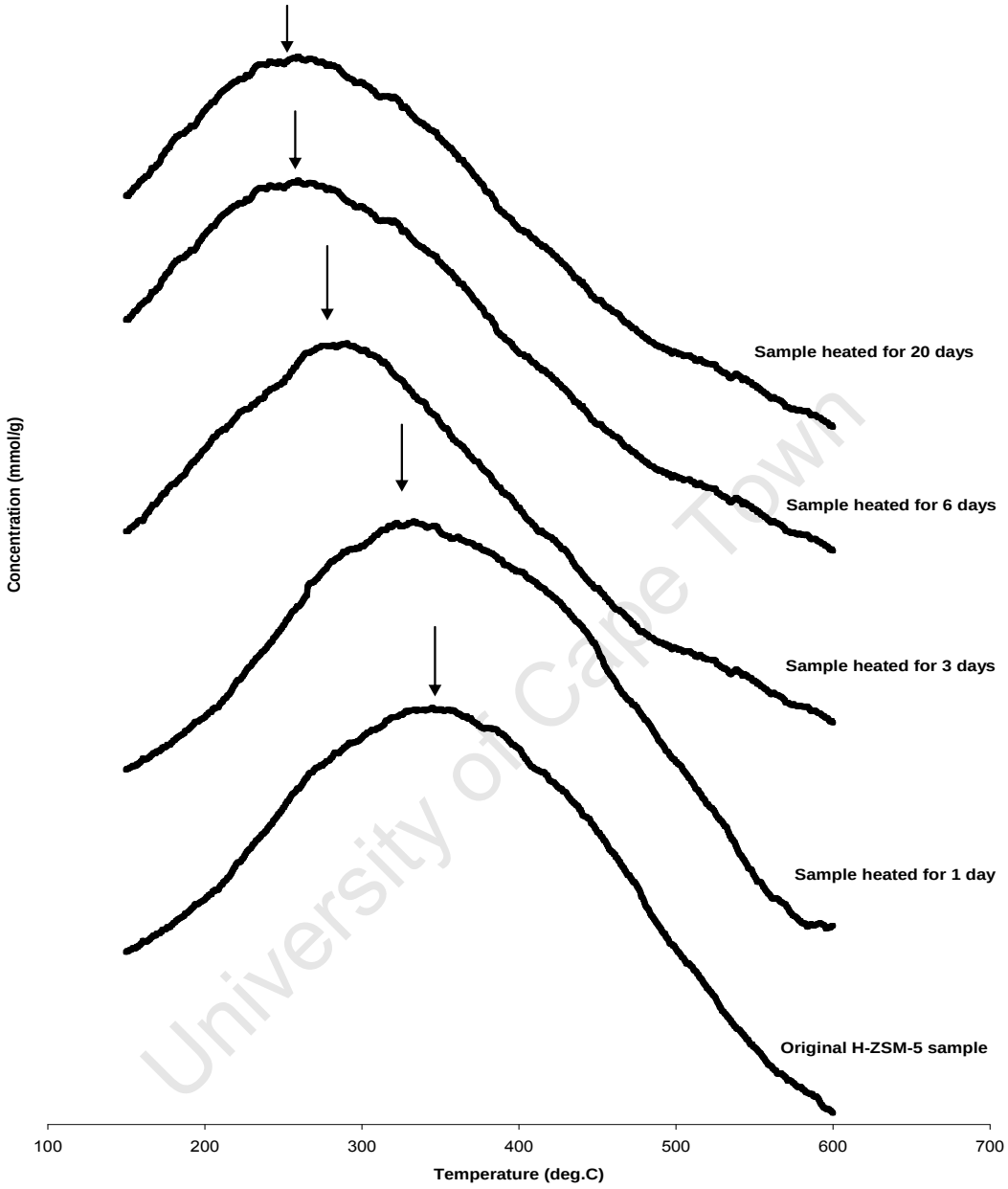

Figure 3.16: TPD-profiles of ZSM-5 samples separated from the combined K-Fe_2O_3/H-ZSM-5 samples after heated at 350oC for various times

Figure 3.17 and Table 3.8 show the amount of ammonia desorbed from ZSM-5 separated from the combined pellet containing K-Fe_2O_3/H-ZSM-5 as a function of heating time at 350^{o}C. The amount of ammonia desorbed decreases with increasing heating time at 350^{o}C, and flattens out for heating times at 350^{o}C larger than 6 days. The decrease in the amount of ammonia desorbed is indicative for a reduction in the number of acid sites. This is expected if potassium migrates from the K-Fe_2O_3 section of the combined pellet to the ZSM-5 section. The flattening out of the decrease in the amount of ammonia desorbed indicates that an equilibrated state has been achieved. It should be noted that the amount of ammonia desorbed does not decrease to 0 mmol/g. Thus, a relative large number of acid sites (ca. 53% of the initial number of acid sites) are still present in the equilibrated state.

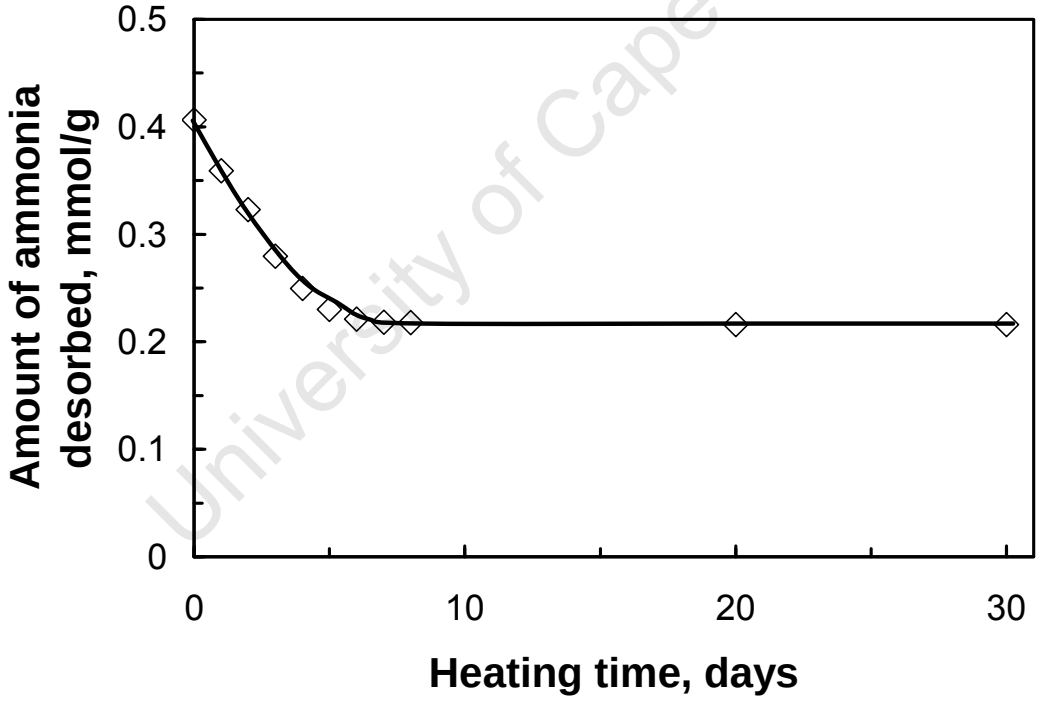

Figure 3.17: Amount of ammonia desorbed during temperature programmed desorption of ammonia adsorbed on ZSM-5 samples separated from the combined K-Fe_2O_3/H-ZSM-5 samples after been heated at 350^{o}C for various times

Table 3.8: The effect of heating time at 350°C of the combined pellet K-Fe_2O_3/H-ZSM-5 on the amount of ammonia desorbed from ZSM-5 separated from the pellet during NH_3-TPD (as determined by integration of the TCD-signal) and the temperature at which the rate of desorption is maximum (T_{max})

$t_{heating}$ (days)	$n_{NH_3,adsorbed}$, mmol/g (TCD)	T_{max} (°C)
0	0.4065	350
1	0.3593	335
2	0.3229	305
3	0.2796	286
4	0.2498	276
5	0.2301	267
6	0.2211	260
7	0.2181	259
8	0.2179	260
20	0.2162	261
30	0.2160	259

The decline in the temperature at which the rate of desorption is maximum as a function of the heating time at 350°C is shown in Figure 3.18 (see also Table 3.8). The change in the temperature at which the rate of ammonia desorption is maximum is due to a reduction in the specific number of acid sites (i.e the acid site per gram of total sample). Several researchers have shown that an increase in the Si/Al ratio lowers the temperature, T_{max}, at which the rate of ammonia desorption is maximum [Hidalgo et al, 1984; Kapustin et al, 1988]. The overall reduction of acid site density results in a reduction in the likelihood of re-adsorption of desorbed ammonia. The peak temperatures were found to decrease from ca. 350°C to 260°C as the heating time increased from 1 day to 30 days.

The change in the temperature at which the rate of ammonia desorption is maximum does not change much after 6 days of heating.

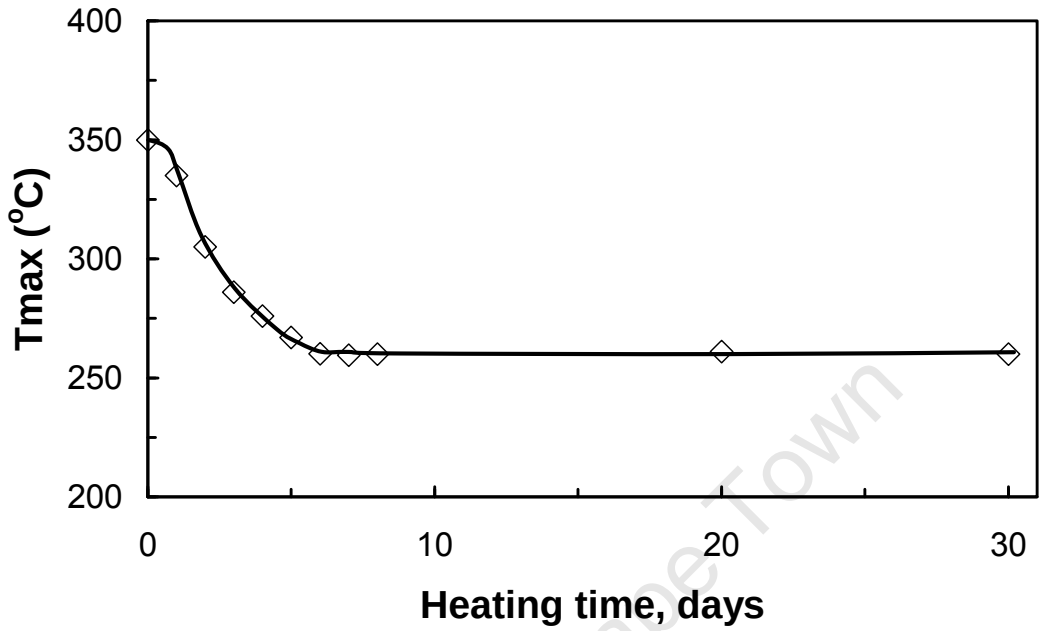

Figure 3.18: Temperature at which the rate of ammonia desorption is the maximum during temperature programmed desorption of ammonia adsorbed on ZSM-5 samples separated from the combined K-Fe_2O_3/H-ZSM-5 samples after been heated at 350°C for various times

4 Discussion

The objective of this study was to develop a methodology for the determination of the migration of potassium in pellets originally containing K-Fe_2O_3 and H-ZSM-5. Hematite crystallites with an average size of ca. 38 nm were synthesized via precipitation in an aqueous iron nitrate solution and subsequent calcination. The addition of potassium in the form of potassium nitrate did not seem to affect the morphology of hematite as evidenced using XRD. The elemental analysis indicated that after calcination for 8 hrs at 350^{o}C potassium nitrate is present on the hematite. This might have been expected since the decomposition temperature of KNO_3 is given as 400^{o}C. Hence, the mobility of potassium originally in the form of KNO_3 was observed in this study.

EDX was chosen as a technique to follow the extent of potassium migration and to monitor the K-concentration profile within the pellet. EDX technique can be used both qualitatively and quantitatively. Accurate quantitative EDX analysis requires uniformity and consistency of data collection conditions, elimination of noise from data, identification of all elements present, and comparison of unknown to standard data with correction for differences of matrix effects [B.J Griffin; C.E Nockolds, 1990]. EDX is better than X-ray mapping and point analysis, since a single line scan yields information with higher statistical relevance. However, quantitative EDX line profile analysis is still a challenge.

EDX-analysis clearly showed that the concentration gradient within either the zone originally containing K/Fe_2O_3 or the zone originally containing H-ZSM-5 is small. The small concentration gradient in potassium in the zone containing originally H-ZSM-5 opened a new route for the determination of the amount of potassium migrated to the zone originally containing H-ZSM-5. Potassium ions neutralize the acid sites in acidic materials.

The determination of the remaining acid sites in H-ZSM-5, e.g. using NH_3-TPD, is therefore an alternative method to determine the amount of potassium migrated to the zone originally containing H-ZSM-5.

A large step in the concentration of potassium was observed around the zone boundary between the zone originally containing K-Fe_2O_3 and the zone originally containing H-ZSM-5. This implies that the process is dominated by mass transfer across the boundary of the zones.

The amount of acid sites in H-ZSM-5 originally in the pellet decreased with time, but seemed to level off after ca. 7 days. The final amount of acid sites still present is ca. 53% of the amounts of acid sited originally present in H-ZSM-5. H-ZSM-5 (Si/Al=40) originally contains 0.41 mmol acid sites per gram. The K/Fe_2O_3 sample contains according to AAS-analysis 1.02 mmol K per gram. The flattening off of the potassium concentration with time is thus not due to depletion of K in the zone originally containing K/Fe_2O_3, but rather due to achieving of an equilibrium situation.

4.1 Mass transfer analysis

The scatter in the data obtained by EDX did not allow a detailed analysis on the rate of mass transfer of potassium in a pellet originally containing K-Fe_2O_3 and H-ZSM-5. On the other hand, the NH_3-TPD data can be used to assess the rate of potassium transfer from the zone originally containing K-Fe_2O_3 to the zone originally containing H-ZSM-5.

It is assumed that the rate of mass transfer is limited by the transfer across the phase boundary within the pellet. This is justified based on the EDX-analysis, which shows a change in the drop of the potassium content across the phase boundary with time, but a negligible concentration gradient within the individual zones at any time.

Thus, the rate of mass transfer is given by:

$$r_{K-transfer} = \frac{dC_{K,H-ZSM-5}}{dt} = k \cdot a \cdot \left(C_{K,H-ZSM-5,eq} - C_{K,H-ZSM-5}\right) \quad (4.1)$$

with

$r_{K\text{-}transfer}$: rate of transfer of K across the phase boundary

$C_{K,H\text{-}ZSM\text{-}5}$: potassium content in the zone originally containing H-ZSM-5

$C_{K,H\text{-}ZSM\text{-}5,eq}$: equilibrium potassium content in the zone originally containing H-ZSM-5 (in equilibrium with a partially depleted zone containing K-Fe_2O_3)

k: mass transfer coefficient

a: mass transfer area

In NH_3-TPD, the remaining acid sites are titrated. The concentration of potassium in the zone originally containing H-ZSM-5 at a given time can be related to the concentration of acid sites in H-ZSM-5 at a given time, if it can be assumed that each potassium ion migrated to the zone originally containing H-ZSM-5 neutralizes one acid site.

$$C_{K,H-ZSM-5} = C_{NH_3,desorbed,H-ZSM-5,t=0} - C_{NH_3,desorbed,H-ZSM-5,t=t} \quad (4.2)$$

Substitution of this condition in equation 4.1 leads to:

$$-\frac{dC_{NH_3,desorbed,H-ZSM-5,t=t}}{dt} = k \cdot a \cdot \left(dC_{NH_3,desorbed,H-ZSM-5,t=t} - dC_{NH_3,desorbed,H-ZSM-5,t=\infty}\right) \quad (4.3)$$

Solving the differential equation:

$$-\ln\left(\frac{C_{NH_3,desorbed,H-ZSM-5,t=t} - C_{NH_3,desorbed,H-ZSM-5,t=\infty}}{C_{NH_3,desorbed,H-ZSM-5,t=0} - C_{NH_3,desorbed,H-ZSM-5,t=\infty}}\right) = k \cdot a \cdot t \quad (4.4)$$

or

$$C_{NH_3,desorbed,H-ZSM-5,t=t} = C_{NH_3,desorbed,H-ZSM-5,t=\infty} + \left(C_{NH_3,desorbed,H-ZSM-5,t=0} - C_{NH_3,desorbed,H-ZSM-5,t=\infty}\right) \cdot e^{-k \cdot a \cdot t} \quad (4.5)$$

Figure 4.1 shows the fit of the amount of ammonia desorbed in the NH_3-TPD of the zeolite in the pellet as a function of time exposed at 350^{o}C. Table 4.1 gives the constants obtained by fitting data to equation 4.5. A good fit of the experimental determined amount of ammonia to the non-linear mass transfer equation 4.5 is obtained. The amount of ammonia desorbed from the fresh, fully exchanged H-ZSM-5, was also determined by fitting (0.416 ± $5.3 \cdot 10^{-6}$ mmol NH_3/g) and is shown to compare favourably with the experimental determined value (0.4065 mmol/g). A lumped constant (k·a) for mass transfer coefficient of 0.370 ± $1.6 \cdot 10^{-5}$ day^{-1} was determined. The amount of ammonia desorbed from H-ZSM-5 in equilibrium with K/Fe_2O_3 was determined to be 0.208 ± $2.8 \cdot 10^{-6}$ mmol NH_3/g.

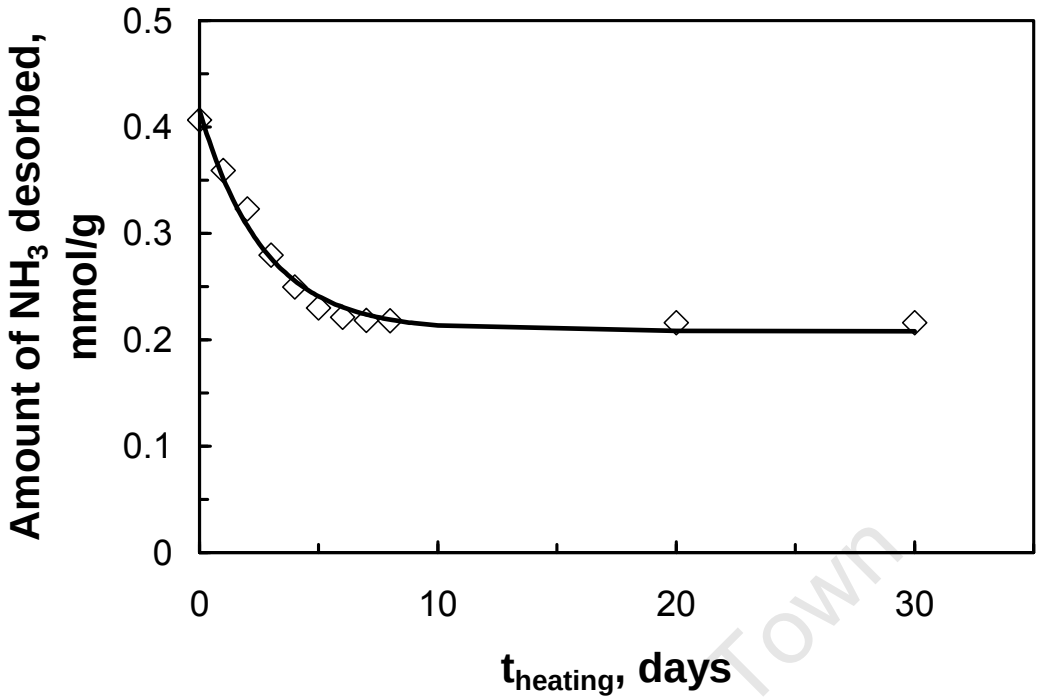

Figure 4.1: Comparison of experimentally obtained amount of ammonia desorbed in NH_3-TPD as a function of heating time in K-Fe_2O_3/H-ZSM-5 pellet with fitted curve according to eq. 4.5

Table 4.1: Fitting parameters to describe the experimentally obtained amount of ammonia desorbed in NH_3-TPD as a function of heating time in K-Fe_2O_3/H-ZSM-5 with equation 4.5

$C_{NH_3,desorbed,H-ZSM-5,t=0}$	$C_{NH_3,desorbed,H-ZSM-5,t=\infty}$	$k \cdot a$	R^2	var.
		day^{-1}		
mmol/g	mmol/g			
$0.416 \pm 5.3 \cdot 10^{-6}$	$0.208 \pm 2.8 \cdot 10^{-6}$	$0.370 \pm 1.6 \cdot 10^{-5}$	0.998	$9.95 \cdot 10^{-5}$

The amount of ammonia desorbed from H-ZSM-5 after heating an infinite time in pellet originally containing K/Fe_2O_3 and H-ZSM-5 implies that at equilibrium 0.208 mmol/g of acid sites are neutralized with potassium upon migration of potassium from the zone originally containing K/Fe_2O_3 to the zone originally containing H-ZSM-5. The pellet originally contained 1 g K/Fe_2O_3 and 1 g H-ZSM-5. Thus, the iron containing zone in the pellet should still contain 80% of the potassium, which was originally in the zone containing K/Fe_2O_3.

The amount of potassium determined to be in the zone originally containing $K\text{-}Fe_2O_3$ using NH_3-TPD is much larger than expected based on Figure 3.15, which was evaluated based on normalized EDX-measurements. There it was implied that ca. 55% of the potassium originally in the $K\text{-}Fe_2O_3$ zone migrated to the zone originally containing H-ZSM-5 (migration of such a large amount of potassium would be sufficient to completely neutralize all acid sited originally present in the pellet). The normalization procedure used implies that the determination using EDX for potassium on iron is as efficient as the determination of potassium on H-ZSM-5, i.e. matrix effects are excluded. Furthermore, it is assumed that the void spaces in the iron phase and in the zeolite zone are identical for all samples. This assumption seems to be invalid.

5 Conclusions and outlook

The migration of potassium in iron/H-ZSM-5 bifunctional system was investigated. For that purpose pellets originally containing zones with K/Fe_2O_3 and H-ZSM-5 were prepared by pressing the material together at 2 tonnes of pressure. The pellets were heated at 350^{o}C in air.

Migration of potassium was visualized using EDX. EDX-profiling showed an approximate equal distribution of potassium in each zone, with a step change over the phase boundary. The step change varied as a function of the heating time. This implies that mass transfer across the phase boundary is the limiting step in the migration of potassium within the pellet. Quantitative evaluation of the potassium profile using EDX failed. This is most likely due to the inhomogeneity of the pellet cross section, i.e. a varying amount of void space within the zones resulted in a large variation in the relative potassium concentration.

Since the EDX technique showed a flat profile within each zone, and thus also in the zone originally containing H-ZSM-5, NH_3-TPD on H-ZSM-5 can be used to determine the amount of potassium neutralizing the acid sites within H-ZSM-5. This would correspond to the amount of potassium migrated across the phase boundary, if all potassium neutralizes the acid sites within H-ZSM-5. Thus, NH_3-TPD can be used to monitor potassium migration under these assumptions.

It was observed, that the amount of ammonia desorbed decreases with increasing heating time at 350^{o}C. The desorption peak in the NH_3-TPD spectra were shifted towards lower desorption temperatures and the peak maximum temperature of the NH_3-TPD are affected by the change in the amount of acid sites present in H-ZSM-5. This is commonly observed in systems affected by re-adsorption of the desorbing compound.

The amount of ammonia desorbed from the zone originally containing H-ZSM-5 with time was fitted to a simple mass transfer model. The mass transfer coefficient was determined to be $0.370 \pm 1.6 \cdot 10^{-5}$ day^{-1}. The mass transfer model predicts that after infinite time only ca. 20% of the potassium originally present on K/Fe_2O_3 would diffuse to the zone originally containing H-ZSM-5, neutralizing ca. 50% of the acid sites originally present.

The work should now be extended to investigate the effect of the pelletizing pressure on the amount of potassium migrating across the phase boundary.

AAS showed that potassium was most likely present as KNO_3. In iron-based Fischer-Tropsch catalysts, potassium is most likely present (depending on the reaction conditions) as K_2O, K_2CO_3 or KOH. Hence, the mobility of potassium in these forms should be investigated.

Furthermore, iron is not present as Fe_2O_3 in the working Fischer-Tropsch catalyst but rather as magnetite or iron carbide. Hence, the migration studies should be performed under conditions favouring the formation of these phases.

REFERENCES

Amenomiya, Y. and Cvetanovic, R. Active Sites of Alumina and silica-alumina as observed by Temperature Programmed Desorption, Journal of Catalysis, vol.18, (1970), 329-337.

Armaroli, T., Simon, L. J., Digne, M., Montanari, T., Bevilacqua, M., Valtchev, V., Patarin, J. and Busca, G, Effect of crystal size and Si/Al ratio on the surface properties of H-ZSM-5 zeolite, Applied Catalysis A, vol.306, (2006), pp. 78 - 84.

Baerlocher, C., McCusker, L. and Olson, D, Atlas of Zeolite Framework Types, (2007)

Botes, F and Bohringer, W, The addition of H-ZSM-5 to the Fischer Tropsch process for improved gasoline production, Applied Catalysis A, vol.267, (2004), pp. 217 - 225.

Botes, F. G, The effect of a higher operating temperature on the Fischer Tropsch / H-ZSM-5 bifunctional process", Applied Catalysis A, vol.284, (2005), pp. 21 - 29.

Butter, S., Chester, A. and Schwartz, A., United States Patent 4298695 to Mobil Oil Corporation (1981).

Corma, A., Corell, C., Fornes, V. and Kolodziejski, Infrared Spectroscopy, thermoprogrammed desorption and nuclear magnetic resonance study of acidity, structure and stability of zeolite MCM-22, vol.15, (7), (1995), pp. 576-582.

Cruciani, G., Zeolite upon heating, factors governing their stability and structural changes, Journal of Physics and Chemistry of solids,vol.67, (9-10), (2006), pp. 1973-1994.

Danziger, M., Hallac, B. and Asscher, M., Surface Diffusion of Potassium Coadsorbed with CO on Ru(001):A Coverage Grating-Optical Second Harmonic Diffraction study, Journal of Physical Chemistry B,vol.108, (2004), pp. 17851-17856.

Davis, B. H., Fischer Tropsch synthesis: relationship between iron catalyst composition and process variables, Catalysis Today, vol.84, (2003), pp. 83 - 98.

Dictor, R. A. and Bell, A. T., Fischer Tropsch synthesis over reduced and unreduced iron oxide catalyst, Catalysis, vol.97, (1), (1986), pp. 121 - 136.

Dry, M., The Fischer Tropsch Synthesis in Catalysis -science and Technology, Springer Verlag, vol.1, (1981), pp. 159-255.

Dry, M., The Fischer Tropsch Process, Elsevier Science Publishers B.V, (1990), pp. 183-206.

Dry, M., Fischer Tropsch reaction and the environment, Applied Catalysis A: General, vol.189, (1991), pp. 185-190.

Dry, M. E., Practical and theoretical aspects of the catalytic Fischer Tropsch process, Applied Catalysis A, vol.138, (1996), pp. 319 - 344.

Dry, M., The Fischer Tropsch process, Catalysis Today, vol.71, (2002), pp. 227-241.

Dry, M.E., Fischer Tropsch Synthesis-Industrial, John Wiley and Sons, 2003, pp. 347.

Eliason, S. A. and Bartholomew, C. H., Reaction and deactivation kinetics for Fischer Tropsch synthesis on unpromoted and promoted iron catalyst, Applied Catalysis A, vol.186, (1999), pp. 229 - 243.

Forni, L., Vatti, F. and Ortoleva, E., Desorption-Diffusion of Ammonia in Molecular Sieves, Journal of Catalysis,vol.12, (1), (1992), pp. 101-106.

Fraenkel, D., Cherniavsky, M. and Levy, M. Proceedings, 8th International Congress on Catalysis, Berlin, Vol IV, 545-554, Dechema, Frankfurt-am-Main, (1984)

Guo, H. and Zaera, F., The reactivity of hydroxyl groups towards ammonia on Ni (110) surface, Surface Science, vol.524, (2003), pp. 1 - 14.

Griffin, B. and Nockolds, C.E. 6th AMAG EDS Micro-analysis school notes, (1990), pp. 1-100.

Haag, W.O, Chen, N.Y, Catalyst Design Progress and Perspectives, John Wiley and Sons (1987).

Hidalgo, C., Itoh, H., Hattori, T., Niwa, M. and Murakami, Y., Measurement of the Acidity of Various Zeolite by Temperature Programmed Desorption of Ammonia, Journal of Catalysis, vol.85, (1984), pp. 362-369.

Horsley, J., Corma, A., Derouane, E. and Guisnet, M., New Zeolite applications in the petroleum and petrochemical industries, Catalytica Studies Division, (1993), pp. 223.

Iwamoto, M., Tajima, M. and Kagawa, S., Journal of Chem.Soc, Chem.Commun, (1986), pp. 598-600.

Kapustin, G., Brueva, T. and Klyachko, A., Determination of the number and acid strength of acid sites in Zeolites by Ammonia adsorption, Applied Catalysis, vol.42, (1988), pp. 239-246.

Kofke, G., Gorte, R. and Farneth, W., Journal of Catalysis, vol.114, (1988), pp. 34-35.

Kofke, T. and Gorte, R., A Temperature Programmed Desorption Study of Olefin Oligomerization in H-ZSM-5, Journal of Catalysis, vol.115, (1989), pp. 233-243.

Lowenthal, E., Schwarz, S. and Foley, H., Analysis of surface acidity, Journal of Catalysis,vol.156, (1), (1995), pp. 96-105.

Luo, M. and Davis, B., Fischer Tropsch synthesis: Group II alkali-earth metals promoted catalysts, Applied Catalysis A: General, vol.246, (2003), pp. 171-181.

Ma, Z., Xu, R., Yang, C., Wei, W., Li, W. and Sun, Y., The effect of iron on the adsorption properties of $CuMnZrO_2$ catalyst studies by Temperature Programmed Desorption and FTIR spectroscopy, Journal of Molecular Catalysis A: Chemical, vol.218, (2), (2004), pp. 133-140.

Martinez, A. and Lopez, C., The influence of ZSM-5 zeolite composition and crystal size on the in situ conversion of Fischer Tropsch products over hybrid catalyst, Applied Catalyst A: General, vol.294, (2005), pp. 251-259.

Maxwell, I. and Stork, W., Chapter 17 Hydrocarbon processing with zeolite, Studies in Surface Science and Catalysis ,vol.137, (2001), pp. 747-819.

Moon, G., The Synthesis and Characterisation of Zeolite Beta, Cape Town (1995).

Muller, K., Deckwer, H. and Ralek, M., Fischer Tropsch synthesis on Polyfunctional manganese/iron-pentasil zeolite catalysis, Studies in Surface Science and Catalysis, vol.12, (1982), pp. 276-274.

Narkiewicz, U., Moszynski, D. and Broslawski, Thermal diffusion of potassium on the modified iron surface, Applied Surface Science, vol.252, (2005), pp. 833-838.

Nelson, H., Lussier, R. and Still, M., An estimate of surface acidity in amorphous catalysts from temperature programmed desorption measurements, Applied Catalysis, vol.7, (1983), pp. 113-121.

Niederberger, H., Time change of activity and selectivity during the conversion of gas that is rich in CO, over an Iron-HZSM-5 composite catalyst, Karlsruhe (1988).

Niemantsverdriet, J.W, Spectroscopy in Catalysis, (2007), Wiley-VCH.

Niu, F. and Hofmann, H, Activity and deactivation behavior of various zeolite catalysts, Applied Catalysis A: General, vol.128, (1995), pp. 107-118.

Ngantsoue-Hoc, W., Zhang, Y., O'Brien, R., Luo, M. and Davis, B., Fischer Tropsch synthesis: activity and selectivity for group I alkali promoted iron-based catalyst", Applied Catalysis A: General, vol.236, (2002), pp. 77-89.

Rajagopal, S., Marzari, J. and Miranda, R., Silica Alumina Supported Mo oxide catalysts, Journal of Catalysis, vol.151, (1), (1995), pp. 192-203.

Raksakoon, C. and Limtrakul, J., Adsorption of aromatic hydrocarbon onto H-ZSM-5 zeolite investigated by ONIOM study", Journal of Molecular Structure, vol.631, (2003), pp. 147 - 156.

Schulz, M., Zhao, S. and Baumgartner, W.,Stud.Surf.Sci. Catalysis,vol.34, (1987), pp. 479-492.

Schulz, H. and Claeys, M., Reaction of alpha olefins of different chain length added during Fischer Tropsch synthesis on a cobalt catalyst in a slurry reactor", Applied Catalysis A: General,vol.186, (1-2,4), (1999), pp. 71-90.

Schulz, H., Niederberger, H., Kneip, M. and Weil, F., Synthesis gas conversion on Fischer Tropsch Iron/HZSM5 composite catalyst, Studies in Surface Science and Catalysis, vol.61, (1991), pp. 313-323.

Schulz, H., Short history and present trends of Fischer Tropsch synthesis, Applied Catalysis A: General, vol.186, (1999), pp. 3-12.

Schulz, H. and Claeys, M.,Reaction of alpha olefins of different chain length added during Fischer Tropsch synthesis on a cobalt catalyst in a slurry reactor, Applied Catalysis A: General, vol.186, (1-2, 4), (1999), pp. 71-90.

Steynberg, A. P., Dry, M. E., Davis, B. H. and Breman, B., Chapter 2 Fischer Tropsch Reactors", Studies in Surface Science and Catalysis,vol.152, (2004), pp. 64-195.

Topsoe, N., Pedersen, K. and Derouane, E., Infrared and Temperature Programmed Desorption study of the Acidic Properties of ZSM-5 Type Zeolite, Journal of Catalysis, vol.70, (1981), pp. 41-52.

Udaya.V, R. G., Bifunctional Catalysis in Syngas Conversions, Catalysis Today, vol.6, (1990), pp. 207.

Vannice, M., The catalysis synthesis of hydrocarbons from H2/CO mixture over the Group VIII metal, Journal of Catalysis ,vol.50, (2), (1977), pp. 228-236.

van Steen-Callanan, L., Methanol Amination over Hydrothermally Treated Zeolites RHO and Mordenite, (1999), Cape Town.

Weber, R., The Characterisation and Elimination of the External Acidity of ZSM-5, (1993), Cape Town.

Weber, R., Fletcher, J., Möller, K. and O'Connor, C., The characterisation and elimination of the external acidity of ZSM-5, Microporous Materials, vol.7, (1), (1996), pp. 15-25.

Westre, E., Brown, D., Kutzner, J. and George, S., Surface diffusion of potassium on Ru(001), Surface Science ,vol.294, (3), (1993), pp. 185-196.

Zhao, W., Kerner, G. and Asscher, M., Interaction and diffusion of potassium on Cr_2O_3(0001)/Cr (110), Physical Review B, vol.62, (11), (2000), pp. 7527-7534.

APPENDICES

Appendix A: XRD reference patterns

XRD studies the structural properties of catalysts and catalytic model surfaces by means of interference effects in scattered radiation. It is one of the most frequently applied techniques for catalyst characterisation. XRD technique is used to identify crystalline phases inside the catalyst by means of lattice structural parameters and to obtain an indication of particle size. The reference patterns of a particular phase of species are in each case matched to the observed peaks. The peaks that cannot be distinguished are in most cases due to overlapping of the peaks and in only a few cases, due to the noise levels in the spectrum.

A.1 Iron oxide

Fe_2O_3 Reference peaks		Observed peaks	
2 Theta	Intensity	2 Theta	Intensity
24.1	30	24.1	70
33.3	100	33.3	100
35.7	70	35.7	80
40.9	20	40.9	70
49.5	40	49.5	70
54.1	45	54.1	80
57.7	8	57.7	40
62.5	5	62.5	70
64.1	10	64.1	80
72.1	6	72.1	40
75.7	8	75.7	30

A.2 H-ZSM-5

H-ZSM-5 Reference peaks		Observed peaks	
2 Theta	Intensity	2 Theta	Intensity
7.9	90	7.9	90
8.8	90	8.8	90
23.9	100	23.9	80
24.3	70	24.3	70
24.8	70	24.8	70

A.1 Potassium promoted Iron oxide

K/Fe_2O_3 Reference peaks		Observed peaks	
2 Theta	Intensity	2 Theta	Intensity
24.03	30	24.03	50
33.02	100	33.02	100
35.45	70	35.45	70
40.79	20	40.79	50
49.21	40	49.21	80
53.88	45	53.88	100
57.16	5	57.16	50
62.25	10	62.25	80
63.68	30	63.68	80
71.40	30	71.40	40
77.54	10	77.54	30

Appendix B: SEM photographs

Scanning electron microscopy (SEM) is one of the most versatile and well known analytical techniques. SEM has advantages that include high magnification, large depth of focus, great resolution and an ease of sample preparation and observation. Electrons generated from an electron gun enter a surface of a sample and generate many low energy secondary electrons. The intensity of these secondary electrons is governed by the surface topography of the sample. The sample surface image is constructed by measuring secondary electron intensity as a function of the position of the scanning primary electron beam.

Electrons are diffracted by particles enabling one to obtain dark filed images together with crystallographic information. These electrons can collide with atoms in the sample and become scattered backwards. Backscattering becomes more effective if the mass of the atom increases. In addition to secondary electrons imaging, backscattered electrons imaging and Energy Dispersive X-ray (EDX) analysis are widely used for chemical analysis. The intensity of backscattered electrons generated by electron bombardment can be correlated to the atomic number of the element within the sampling volume. The characteristic X-rays emitted from the sample serve as fingerprints and give elemental information of the samples including semi-quantitative analysis, quantitative analysis, line profiling and spatial distribution of elements. Hence, qualitative elemental information can be revealed.

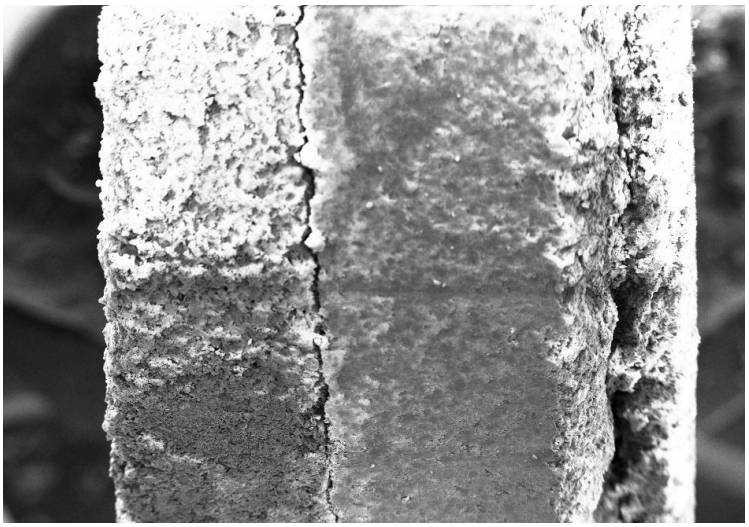

Figure 6.1: SEM photograph showing a picture of two pellets which have been pressed together to form a single pellet.

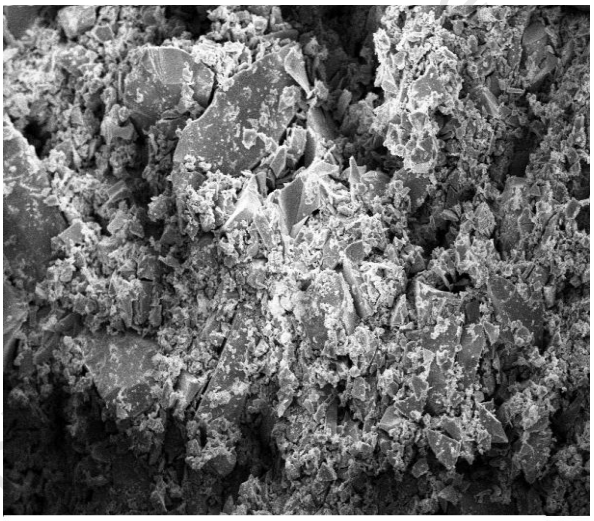

Figure 6.2: SEM photograph of potassium promoted iron oxide.

Appendix C: EDS Plots

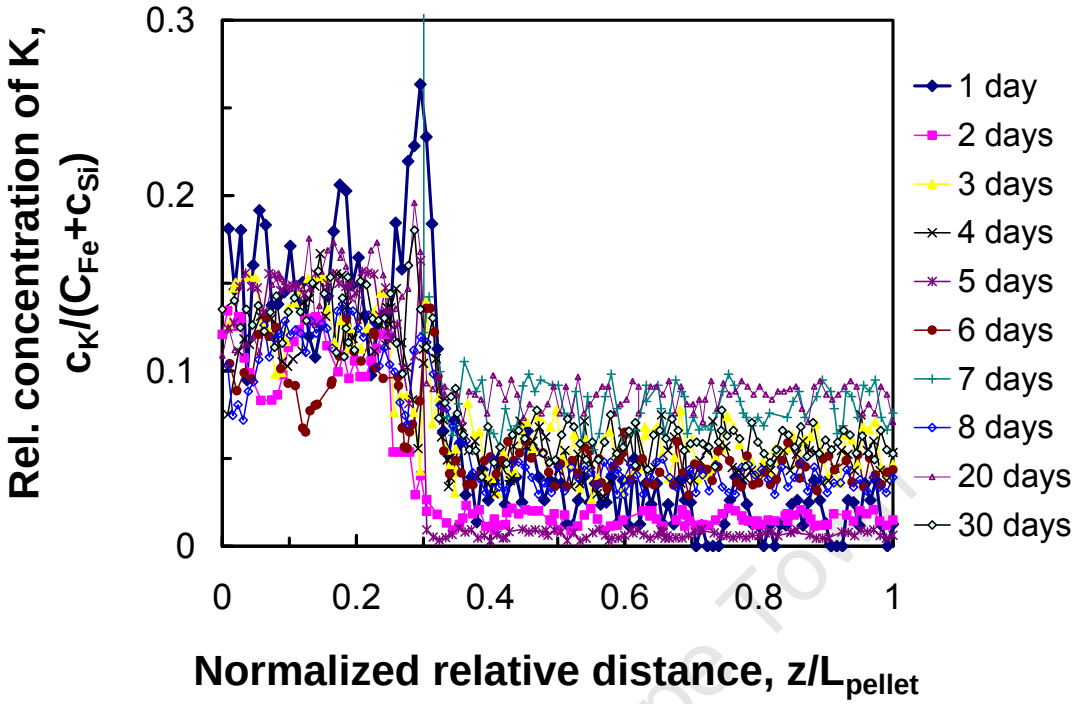

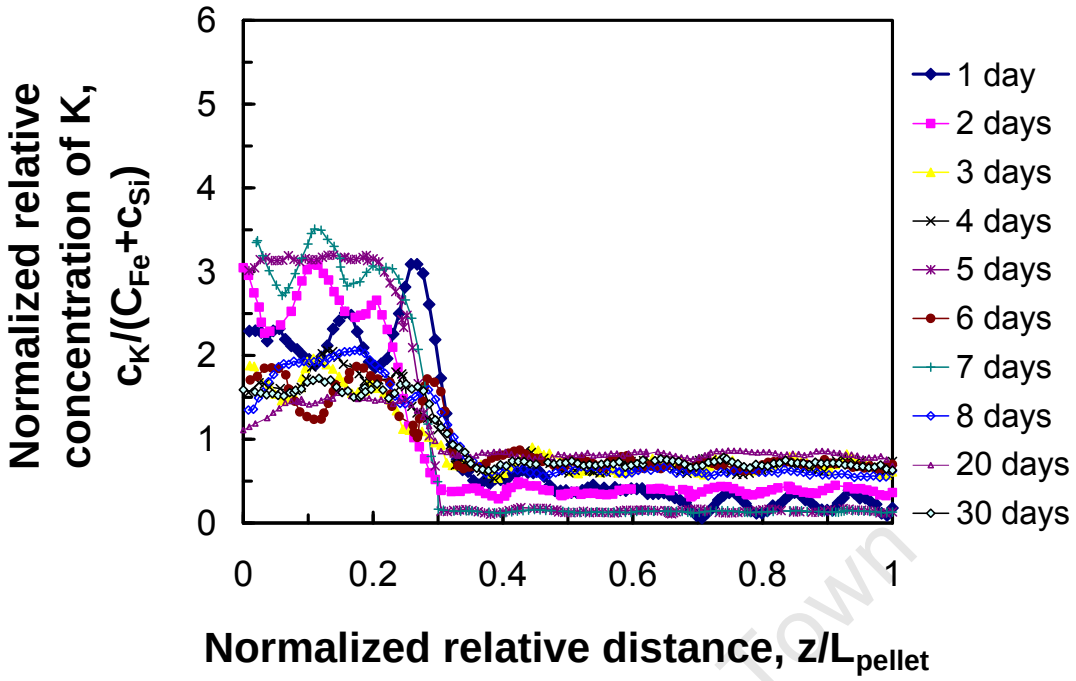

Figure 6.3: Normalized concentration profile of K relative to Fe and Si as a function of normalized relative length of pellet after various times of heating at 350°C (length of pellet normalized relative to a fixed boundary between the zone, which originally contains K-Fe_2O_3, and the zone, which originally contains H-ZSM-5, at z/L_{pellet} = 0.3)

Appendix D: NH_3- TPD

Temperature-Programmed Desorption (TPD) is one of the most widely used powerful surface techniques for investigating the strength, amount and the structure of the acid sites in zeolites. TPD is considered to be a potential technique for measuring the amount and the distribution of the active site. Although it has the drawbacks of being dependent on the experimental conditions such as the rate of temperature increments, equilibrium temperature, but the Brønsted-acid site density is usually one of the most crucial parameters [Hidalgo, et al, 1984]. But when it was compared to other similar desorption techniques for measuring the distribution of acid site distribution is was found to be less time intensive since it only analyse fully saturated surfaces and it uses only one desorption rate.

Numerous catalysts have been investigated using the temperature desorption technique, such as alumina [Amenomiya and Cvetanovic, 1970], silica-alumina [Nelson et al, 1983], [Amenomiya and Cvetanovic, 1970], mordenite [Kapustin et al, 1988] and ZSM-5 [Kofke et al, 1988; Topsoe et al, 1981; Kapustin et al, 1988; Hidalgo et al, 1984]. The probe which was used included ammonia [Hidalgo et al, 1984; Kapustin et al, 1988; Topsoe et al, 1981], pyridine [Topsoe et al, 1981], alkenes [Amenomiya and Cvetanovic, 1970; Kofke et al, 1988].

The desorption spectrum is a plot of desorption rate versus temperature; this plot can consist of one or more peaks, which identify specific site on the catalyst surface. By using suitable calibrated thermal conductivity detectors, flame ionization detectors, mass spectrometers or titration methods, one can determine the amount of material desorbed. In cases whereby bases are desorbed from the acid catalyst, this can be related to the number of acid sites on the catalyst surface. Thus a distribution of acid site strength with respect to temperature as well as the desorption activation energy can be obtained [Amenomiya and Cvetanovic, 1970].

Iwamoto et al. (1986), together with Kapustin et al. (1988) found that the aluminium content influenced the peak maximum temperature, but in they founding they discovered that the structure had no effect. Its can be concluded that the peak maximum temperature cannot be used for the comparison of acid site strengths of different zeolites. According to Forni et al. (1992) the change in peak maximum temperature of desorption spectrum can be influenced by the difference in Si/Al ratios as well experimental conditions (catalyst mass, heating rates, and carrier gas flow rates). An increase in carrier gas flow rate or a decrease in catalyst mass results in lower value of T_{max} of NH_3-TPD spectrum [Kapustin et al, 1988].

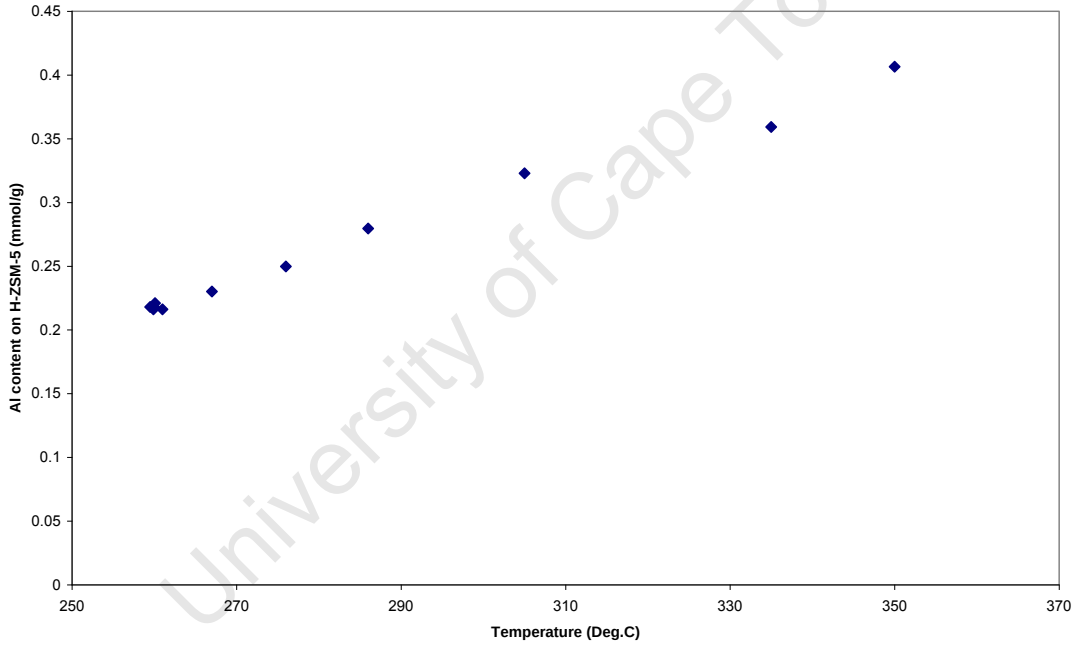

Figure 6.4: Temperature at which the rate of Al is maximum during temperature programmed desorption of ammonia adsorbed on ZSM-5 samples separated from the combined K-Fe_2O_3/H-ZSM-5 samples after heated at 350^{o}C for various times

TPD analysis

The activation energy of desorption is given by the Redhead method:

$$E_{des} = RT_{\max}[\ln(\frac{\nu T_{\max}}{\beta}) - 3.46]$$

Where:

E_{des} activation energy of desorption

R gas constant

$T_{\max}$ peak maximum temperature

ν pre-exponential factor

β heating rate, $\frac{dT}{dt}$

This equation is correct for first order desorption. It's mainly applied to determine E_{des} from a single TPD spectrum. The critical point of this equation is that the general choice of ν should be 10^{13} s^{-1}, which is independent of coverage. This value is chosen when there is a small chance of entropy between the molecule in the ground state and the transition state. This equation can only be used if there is a reliable value of the prefactor is available [J.W Niemantsverdriet, 3rd edition]

Appendix E: ***Expected concentration profile of potassium using Diffusion constant.***

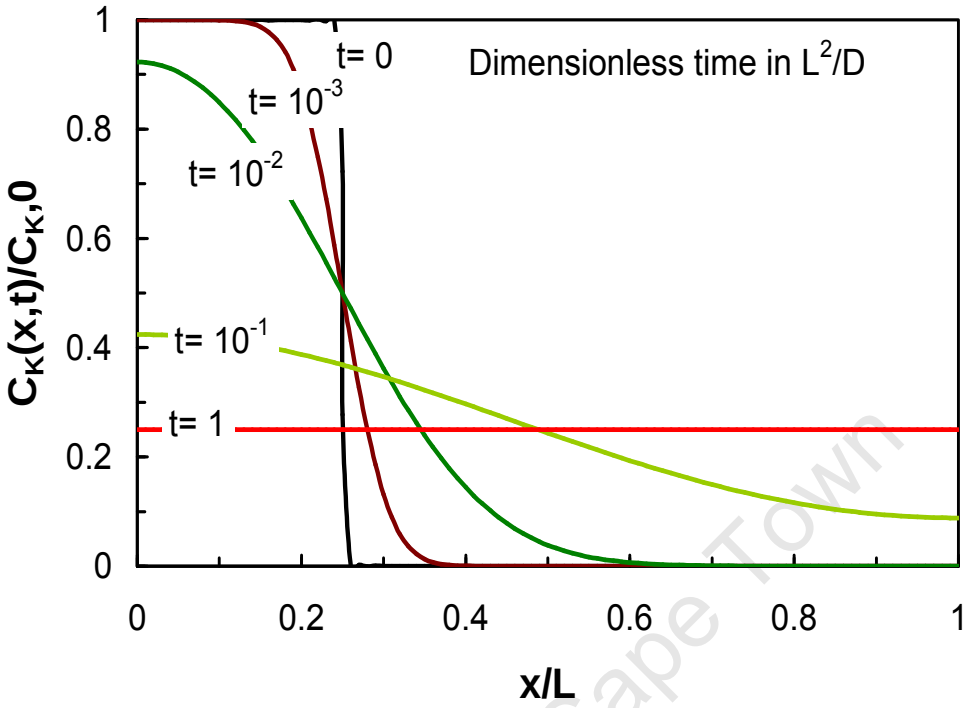

Figure 6.5: Expected concentration profiles of potassium in a homogeneous block (the initial fraction of the length containing potassium was 0.25)

Figure 6.5 shows the expected concentration profile of potassium as a function of the position in the block. The curves were computed assuming that the part containing the potassium initially is 0.25 of the total length of the block. Thus the curves depend on the time evolved since the start of the experiment (time is here taken as a relative measure of L^2/D). The diffusion coefficient is best measured at times between 10^{-2} and 10^{-1} L^2/D. The measurement will entail measuring the concentration profile as a function of x/L and fit the curve to a value of L^2/D. Therefore diffusion coefficient D can be obtained by knowing L.

Appendix F: Comparison of techniques

Comparison of the amount of acidity (mmol/NH_3/g catalyst) obtained using NH_3-TPD after heating the pellets with those obtained using EDX and AAS techniques can be seen in appendix D. Results show that equivalent amount of potassium where adsorbed for H-ZSM-5, thus concluding that EDX and AAS can be use in correlation with NH_3-TPD to monitor potassium migration, since similar results were obtained. All three characterisation techniques (NH_3-TPD, AAS and EDX) indicated no change in the acidity of H-ZSM-5 sample after 6 days of heating at 350^oC. The acidity ratio calculated for the zeolite obtained from all three characterisation techniques showed to be approximately the same irrespective of how long it was exposed to heat after 6 days of heating.

A decrease in the acidity with increasing potassium for H-ZSM-5 may be due to potassium interacting with H^+ in the zeolite, thus decreasing the acidity of the zeolite. As the NH3-TPS, EDX and AAS data do not indicate a change in the acidity of H-ZSM-5 after 6 days it can be concluded that the internal acidity is not affected by the deposition of K and that the pore volume remains the same. The boundary layer could have an effect on the rate of diffusion of potassium. It could be that most of the potassium from the iron catalyst does not reach potassium and get stuck on the boundary layer, thus saturation will not be reached between these two catalysts.

The other reasoning that can be made is that since ZSM-5 has H^+ ion exchange between K^+ will take place, depending on where the H^+ will be on the structure, ion exchange will continue to take place until the whole surface of the zeolite is covered with positively charged K. Thereafter the surface of the zeolite will be positively charge thus resulting in potassium to no longer diffuse into ZSM-5, because of repulsion that will take place when positive charges come into contact.

This therefore results in the saturation being reached in the ZSM-5 catalyst after 6 days, whereby diffusion of potassium can no longer take place, thus the amount of Al will be constant after 6 days. These results were confirmed by all the characterisation techniques that were used for experiments. From Figure 4.2 which shows the mass transfer coefficients for the concentrations of potassium as a function of time, its can be observed that, there is mass transfer, but it can be negligible, since the values are relatively small.